

Carla Corrêa Mendes Gouvêa

*AVALIAÇÃO ANTIBIOFILME E
ANTICARIOGÊNICA DE NANOCOMPÓSITOS
FORMADOS POR POLIFOSFATOS DE SÓDIO E
FLÚOR ASSOCIADOS À NANOPARTÍCULAS
DE PRATA. ESTUDO IN VITRO*

ARAÇATUBA - SP

2018

Carla Corrêa Mendes Gouvêa

Avaliação antibiofilme e anticariogênica de nanocompósitos formados por polifosfatos de sódio e flúor associados à nanopartículas de prata. Estudo in vitro

Tese apresentada à Faculdade de Odontologia do Campus de Araçatuba – UNESP, para obtenção do Grau de “Doutora em Ciência Odontológica” - Área de Concentração Saúde Bucal da Criança.

Orientadora: Profa. Ass. Dra. Debora de Barros Barbosa

**Co-orientadoras: Profa Dra Marcelle Danelon e
Dra Jackeline Gallo do Amaral**

**ARAÇATUBA – SP
2018**

Catálogo-na-Publicação

Diretoria Técnica de Biblioteca e Documentação – FOA / UNESP

G719a

Gouvêa, Carla Corrêa Mendes.

Avaliação antibiofilme e anticariogênica de nanocompósitos formados por polifosfatos de sódio e flúor associados à nanopartículas de prata : estudo in vitro / Carla Corrêa Mendes Gouvêa. - Araçatuba, 2018

80 f. : il. ; tab.

Tese (Doutorado) – Universidade Estadual Paulista,
Faculdade de Odontologia de Araçatuba

Orientadora: Debora de Barros Barbosa

Coorientadora: Marcelle Danelon

Coorientadora: Jackeline Gallo do Amaral

1. Polifosfatos 2. Cárie dentária 3. Biofilmes 4. Prata
5. Nanopartículas 6. Desmineralização do dente I. T.

Black D27

CDD 617.645

Dedicatória

À Deus,

por ter me protegido e iluminado durante toda a vida.

Aos meus pais, Ivonete e José Carlos,

obrigada por todo amor e apoio. Mãe, sem você eu não teria chegado até aqui. Ter cuidado das meninas me deu a tranquilidade necessária para seguir em frente no doutorado. Pai, sua inteligência e conhecimento sempre me nortearam a buscar o máximo que pude. Amo muito vocês!

Ao meu marido Afranio,

sem seu apoio e compreensão nada disso seria possível. Sempre me incentivou a lutar pelos meus objetivos. Obrigada pelo amor mesmo diante de uma esposa cansada e estressada. Nos dias que virão espero recompensar esses anos difíceis. Peço a Deus que abençoe a nossa família. Você é o amor da minha vida!

Às minhas filhas Maria Luíza e Marina,

obrigada por serem a luz da minha vida. Por vocês quero ser sempre melhor e quero criá-las da melhor maneira possível. Me desculpem pela ausência nesses anos, mas se errei foi pensando em um dia dar o melhor pra vocês! Mamãe as ama infinitamente!

Aos meus sogros Afranio e Virgínia,

e também minhas cunhadas Amaralina e Aline, meus cunhados Bruno e Marcelo e meus sobrinhos Marcelinho, Eduarda, Pedro, Paolla, Mateus e Gabriela, sem vocês eu não teria conseguido. Obrigada pela força, compreensão e carinho que sempre me

motivaram a continuar nos estudos. Vocês são muito importantes na minha vida.

À toda minha família, avós (in memoriam) tios e primos, em especial aos meus tios José Márcio e Cássia, por me amarem, rezarem e torcerem por mim. Vocês dois fazem parte dessa conquista!

AGRADECIMENTO ESPECIAL

À minha orientadora, Professora Doutora Débora de Barros Barbosa, obrigada por seus ensinamentos, não só acadêmicos como religiosos. Admiro muito sua inteligência, mas principalmente sua caridade e amor ao próximo que desde o início do curso de doutorado pude presenciar. Agradeço imensamente o respeito e paciência por minhas limitações. Hoje entendo que a nossa convivência foram essenciais para o meu crescimento acadêmico e pessoal. Peço a Deus que lhe abençoe sempre.

Às minhas co-orientadoras, Marcelle Danelon e Jackeline Gallo do Amaral, agradeço à imensa dedicação em me ajudar. É impossível quantificar a minha gratidão por vocês! Sempre estiveram ao meu lado no dia-a-dia, me ensinando e ajudando à executar diversos experimentos tão difíceis. Tenho muito orgulho por ter sido orientada por pessoas de sucesso ascendente e ao mesmo tempo tão humanas.

Ao Professor Titular, Alberto Carlos Botazzo Delbem, obrigada por ter me dado a oportunidade de concretizar meu sonho de fazer doutorado, quando abriu as portas da Odontopediatria para mim em 2013. Nunca me esquecerei disso! Também agradeço muito ao suporte dado aos meus experimentos, sem a sua ajuda nada seria possível. Seu grande conhecimento me estimularam a ser uma aluna melhor.

AGRADECIMENTOS

À Faculdade de Odontologia de Araçatuba-UNESP, nas pessoas do Diretor Prof. Titular Wilson Roberto Poi e Vice-Diretor Prof. Titular João Eduardo Gomes Filho.

Ao Curso de Pós-Graduação em Ciência Odontológica da Faculdade de Odontologia de Araçatuba - UNESP, na pessoa de seu coordenador Prof. Adj. Luciano Tavares Angelo Cintra.

Aos professores da Disciplina de Odontopediatria da Faculdade de Odontologia de Araçatuba-UNESP, Prof. Tit. Robson Frederico Cunha, Prof^a. Tit. Cristiane Duque, Prof. Tit. Juliano Pellin Pessan, Prof. Tit. Célio Percinoto, Prof^a. Tit. Sandra Maria Herondina Coelho Ávila de Aguiar, Prof^a Ass. Dr^a. Rosangela Santos Nery obrigada pelo aprendizado e atenção desde a graduação. Sou muito grata por tudo e lhes admiro muito!

À amiga Líliana, nossa parceria foi especial. Juntas enfrentamos as dificuldades, me passou tranquilidade e segurança quando precisei. Aprendi muito com você! Agradeço muito sua generosidade em me ajudar sempre!

Aos colegas de Pós-graduação José Antônio, Isabel, Jorge, Mayra, Nayara, Karina, Thamires, Thayse, Mariana, Marjully, Caio, Vanessa, Jesse, Laís, Ana Paula pela amizade, ajuda e ensinamentos. Torço muito pelo sucesso de vocês!

*Aos colegas de Pós-graduação **Renan e Gabriela**, que por várias vezes disponibilizaram seu tempo pra me ensinar e também executar os ensaios microbiológicos. Sempre serei agradecida por toda ajuda!*

*À todos os **professores** da graduação e da pós-graduação da Faculdade de Odontologia de Araçatuba-UNESP, os quais são responsáveis pela minha formação acadêmica.*

*Aos técnicos da disciplina de Odontopediatria da Faculdade de Odontologia de Araçatuba - UNESP, **Mário e Ricardo**, pela ajuda e respeito.*

*Às funcionárias da Seção de Pós-Graduação da Faculdade de Odontologia de Araçatuba-UNESP, **Valéria, Lílian, Cristiane** pela atenção e paciência.*

*Aos funcionários da Faculdade de Odontologia de Araçatuba-UNESP, por serem tão prestativos e carinhosos comigo desde a graduação. Em especial ao **Luizinho, Ilídio, Maria Bertolina, Marquinho, Magda, Niltinho**.*

*À Coordenação de Aperfeiçoamento de Pessoal de Nível Superior, **Capes**, pelo apoio financeiro.*

*À equipe do Prof. **Emerson Camargo**, em especial ao pós-doutorando **Francisco**, que me ajudou muito nas análises de microscopia, estando sempre disposição quando precisei. Muito Obrigada Chico!*

À Universidade Federal de São Carlos, UFSCAR, por disponibilizar o LIEC do Departamento de Química e também o microscópio Zeiss Supra 35VP para a realização de algumas etapas do meu projeto de doutorado.

À todas minhas amigas, a amizade com vocês me ajudou a descontraír e esquecer das tensões do dia-a-dia.

Aos amigos Mariana e Lucas, pelo carinho e companheirismo em todos os momentos.

Epígrafe

“Talvez não tenha conseguido fazer o melhor, mas lutei para que o melhor fosse feito. Não sou o que deveria ser, mas Graças a Deus, não sou o que era antes.”

(Marthín Luther King)

Mendes-Gouvêa CC. **Avaliação antibiofilme e anticariogênica de nanocompósitos formados por polifosfatos de sódio e flúor associados à nanopartículas de prata. Estudo *in vitro*.**[Tese]. Araçatuba: Universidade Estadual Paulista; 2018.

RESUMO GERAL

O objetivo deste estudo foi sintetizar e caracterizar nanocompósitos formados por polifosfatos (trimetafosfato de sódio (TMP) ou hexametafosfato de sódio (HMP)) e flúor (F) associados à nanopartículas de prata. Esses nanocompósitos foram avaliados quanto à sua ação anti-biofilme de *Candida albicans* (ATCC 10231) e *Streptococcus mutans* (ATCC 25175) e seu potencial em inibir a desmineralização do esmalte dentário por meio de ensaio *in vitro* de ciclagem de pH. As nanopartículas de prata foram sintetizadas através da redução do nitrato de prata (1 ou 10%) pelo borihidreto de sódio (NaBH₄) em meio isopropílico contendo trimetafosfato de sódio (TMP) ou hexametafosfato de sódio (HMP) e flúor (F). Os nanocompósitos foram caracterizados por microscopia eletrônica de varredura (MEV) e por difração de raios-X, e também determinada a concentração inibitória mínima (MIC) contra células planctônicas de *C. albicans* e *S. mutans*. A efetividade contra biofilmes pré-formados de 24h dos nanocompósitos, foi testada em concentrações de 1x e 10x os valores de MIC (de 40µg Ag ml⁻¹), avaliada através da quantificação de células cultiváveis (CFUs), da atividade metabólica (XTT) e da biomassa total (Cristal Violeta). Os nanocompósitos contendo 10% de Ag apresentaram maior efetividade antimicrobiana contra ambos os microrganismos, comparados aos nanocompósitos contendo 1% de prata. O biofilme de *S. mutans* foi mais suscetível aos nanocompósitos TMP ou HMP/AgNP que o biofilme de *C. albicans*, com reduções respectivas de 2,88-3,71 log₁₀ e 0,45-1,43 log₁₀. Os nanocompósitos permitiram uma diminuição de cerca de 75% da biomassa total e em torno de 90% da atividade metabólica em ambos os biofilmes. Para avaliação *in vitro* do potencial anticárie, foi sintetizado um novo nanocompósito contendo 0,2% de TMP, 100 ppm de flúor e 10% de Ag e caracterizado por

microscopia eletrônica de transmissão (MET). Blocos de esmalte bovino (4 mm x 4 mm, n = 60) selecionados pela dureza superficial inicial (SHi) foram alocados em cinco grupos (n = 12): água deionizada (Placebo), 100 ppm F (100F), 225 ppm F (225F), 100 ppm F + 0,2% TMP (100F/TMP) e 100 ppm F + 0,2% TMP + 10% Ag (100F/TMP/Ag). Os blocos foram tratados 2x ao dia com as soluções e submetidos a cinco ciclos de pH (soluções des e remineralizadora) à 37° C. Em seguida, determinou-se a dureza superficial final (SHf) e a dureza subsuperficial integrada (Δ KHN), e a concentração de fluoreto (F) e cálcio (Ca) no esmalte. A efetividade desse nanocompósito (100F/TMP/Ag) contra a formação de biofilmes simples e misto de *C. albicans* (ATCC 10231) e *S. mutans* (ATCC 25175) foi avaliada por meio da contagem de unidades formadoras de colônias (CFUs). Os biofilmes foram também analisados por microscopia eletrônica de varredura (MEV). A dureza superficial (% SH) foi similar nas amostras tratadas com soluções contendo 225F, 100F/TMP e 100F/TMP/Ag ($p > 0,001$). Além disso, a capacidade de reduzir o corpo da lesão (Δ KHN) foi maior em 110F, 225F, 100F/TMP e 100F/TMP/Ag ($p < 0,001$) na área A (5-20 μ m) e na área B somente com 225F e 100F/TMP. O grupo 100F/ TMP/Ag apresentou maior desmineralização na área B (20-130 μ m) ($p < 0,001$). A concentração de F da solução 100F/TMP/Ag foi semelhante a 225F ($p < 0,001$). Os grupos 100F, 225F, 100F/TMP e 100F/TMP/Ag apresentaram a maior e similar concentração de Ca ($p > 0,001$). A dureza superficial (% SH) foi similar nas amostras tratadas com soluções contendo 225F, 100F / TMP e 100F / TMP / Ag ($p > 0,001$). Além disso, a capacidade de reduzir o corpo da lesão (Δ KHN) foi maior em 110F, 225F, 100F / TMP e 100F / TMP / Ag ($p < 0,001$) na zona A (5-20 μ m) e na zona B apenas com 225F e 100F / TMP. O grupo 100F / TMP / Ag apresentou maior desmineralização na zona B (20-130 μ m) ($p < 0,001$). A concentração de F da solução 100F / TMP / Ag foi semelhante a 225F ($p < 0,001$). Os grupos 100F, 225F, 100F / TMP e 100F / TMP / Ag apresentaram a maior e a mesma concentração de Ca ($p > 0,001$). Embora a solução 100F/TMP/Ag tenha apresentado valores mais baixos de áreas profundas do que a solução contendo 225 ppm F, o nanocompósito foi capaz de inibir a desmineralização da superfície do esmalte. Estes nanocompósitos demonstraram atividade antimicrobiana significativa, especialmente contra *S. mutans*, e podem ser considerados uma alternativa

potencial para novos biomateriais odontológicos, visando a prevenção ou tratamento de lesões cariosas.

Palavras-chave: Polifosfatos; Nanopartículas de prata; Biofilmes; Cárie dentária; Desmineralização do dente.

Mendes-Gouvêa CC. **Antibiofilm and anticariogenic evaluation of nanocomposites formed by fluoride and sodium polyphosphates associated with silver nanoparticles. *In vitro* study.**[Thesis] Araçatuba: UNESP - São Paulo State University; 2018.

GENERAL ABSTRACT

The aim of this study was to synthesize and characterize nanocomposites formed polyphosphates (sodium trimetaphosphate (TMP) or sodium hexametaphosphate (HMP)) and fluoride (F) associated with silver nanoparticles. The anti-biofilm activity of the nanocomposites were evaluated against *Candida albicans* (ATCC ATCC 10231) and *Streptococcus mutans* (ATCC 25175) . as well as their potential in inhibiting demineralization and increasing the remineralization of dental enamel by in vitro pH cycling assay. Silver nanoparticles were synthesized by reduction of silver nitrate (1 or 10%) by sodium borohydride (NaBH₄) in isopropyl medium containing sodium trimetaphosphate (TMP) or sodium hexametaphosphate (HMP)) and fluoride (F). The nanocomposites were characterized by scanning electron microscopy (SEM) and X-ray diffraction. The minimum inhibitory concentration (MIC) of the nanocomposites was determined against planktonic cells of *C. albicans* and *S. mutans*. Effectiveness of preformed 24-hour biofilms of nanocomposites at 1x and 10x MIC values was assessed by quantifying viable cells (CFUs), metabolic activity (XTT) and total biomass (Crystal Violet). The nanocomposites containing 10% Ag showed higher antimicrobial effectiveness against both microorganisms compared to nanocomposites containing 1% silver. The *S. mutans* biofilm was more susceptible to the TMP or HMP-AgNP nanocomposites than the *C. albicans* biofilm, with respective reductions of 2.88-3.71 log₁₀ and 0.45-1.43 log₁₀. The nanocomposites allowed a reduction of about 75% of the total biomass and about 90% of the metabolic activity in both biofilms. For the in vitro evaluation of the anticaries potential, a new nanocomposite containing 0.2% TMP, 100 ppm fluorine and 10% Ag was synthesized and characterized by transmission electron microscopy (TEM). Bovine enamel blocks (4 mm x 4 mm, n = 60) selected by initial surface hardness (SHi) were allocated in five groups (n=12): deionized water (Placebo), 100 ppm F (100 F), 225 ppm F (225 F), 100 ppm F + 0.2% TMP (100 F / TMP)

and 100 ppm F + 0.2% TMP + 10% Ag (100F / TMP / Ag). The blocks were treated 2x daily with the solutions and subjected to five pH cycles (deismineralizing and remineralizing solutions) at 37 ° C. Then, the final surface hardness (SHf) and integrated subsurface hardness (Δ KHN), the concentration of fluoride (F) and calcium (Ca) in the enamel was determined. The effectiveness of this nanocomposite (100F / TMP / Ag) against the formation of single and mixed biofilms of *C. albicans* (ATCC 10231) and *S. mutans* (ATCC 25175) was evaluated by the counting colony forming units (CFUs). Biofilms were also analyzed by scanning electron microscopy (SEM). Similar values of %SH were observed for groups 225F, 100F/TMP and 100F/TMP Ag ($p > 0.001$). The 225F, 100F/TMP and 100F/TMP/Ag solutions showed capacity to reduce the lesion body (Δ KHN) in the depth of 5-20 μ m. F concentration was similar in the enamel for the 100F/TMP/Ag and 225F ($p > 0.001$). The groups 100F, 225F, 100F/TMP and 100F/TMP/Ag presented the highest and the same concentration of Ca ($p > 0.001$). In relation to viable cells 100F/TMP/Ag nanocomposite promoted significant log reductions in the number of CFUs of *S. mutans*, of 5.42 and 4.46 \log_{10} respectively in single and mixed biofilms and *C. albicans* was more resistant. SEM images confirmed these results. The surface hardness (% SH) was similar in the samples treated with solutions containing 225F, 100F/TMP and 100F/TMP/Ag ($p > 0.001$). In addition, the ability to reduce the lesion body (Δ KHN) was greater in 110F, 225F, 100F / TMP and 100F/TMP/Ag ($p < 0.001$) in zone A (5-20 μ m) and in zone B only with 225F and 100F/TMP. The 100F/TMP/Ag group showed greater demineralization in zone B (20-130 μ m) ($p < 0.001$). The F concentration of the 100F/TMP/Ag solution was similar to 225F ($p < 0.001$). Groups 100F, 225F, 100F/TMP and 100F/TMP/Ag showed the highest and the same concentration of Ca ($p > 0.001$). Although the 100F/TMP/Ag solution yielded lower values of lesion deep areas than the solution containing 225 ppm F, but the nanocomposite was able to inhibit demineralization of surface of enamel. These compounds have demonstrated significant antimicrobial activity, especially against *S. mutans*, and can be considered a potential alternative for new dental biomaterials, aiming at the prevention or treatment of carious lesions.

Keywords: Polyphosphates; Silver nanoparticles; Biofilms; Dental caries; Tooth demineralization.

LISTA DE FIGURAS

Capter 1: Sodium trimetaphosphate and hexametaphosphate impregnated with silver nanoparticles: characteristics and antimicrobial efficacy

Figure 1 - XRD patterns of commercial TMP (a) and HMP powder (b) and the synthesized nanocomposites, respectively.....24

Figure 2 - SEM images and EDX mapping in 2-D at different magnifications of T10 (a and b) and H10 (c and d). Arrows indicate AgNP dispersed on TMP and HMP surfaces. Red dots show silver distribution on phosphates.....25

Figure 3 - a) Logarithm (mean \pm dp) of colony forming units normalized by adhesion area (\log_{10} CFU cm^{-2}); (b) absorbance values per cm^2 obtained through crystal violet assay; (c) absorbance values per cm^2 obtained through XTT assay for *C. albicans* and *S. mutans* biofilms after treatment for 24 h. Bars indicate SD of the mean. Different lowercase letters represent statistical difference between groups and concentrations tested (Fisher, $p < 0.001$). NC=negative control; PC=positive control (CHG); T10=TMP-AgNP10%; H10=HMP-AgNP10%.....26

Figure 4 - SEM images of *C. albicans* biofilms: (a) negative control; (b) positive control; (c) T10 ($10 \mu\text{gAg ml}^{-1}$); (d) T10 ($100 \mu\text{gAg ml}^{-1}$); (e) H10 ($10 \mu\text{gAg ml}^{-1}$); (f) H10 ($100 \mu\text{gAg ml}^{-1}$).....27

Figure 5 - SEM images of *S. mutans* biofilms: (a) negative control; (b) positive control; (c) T10 ($40 \mu\text{gAg ml}^{-1}$); (d) T10 ($400 \mu\text{gAg ml}^{-1}$); (e) H10 ($40 \mu\text{gAg ml}^{-1}$); (f) H10 ($400 \mu\text{gAg ml}^{-1}$).....28

Capter 2: *In vitro* evaluation of a composite containing sodium trimetaphosphate, fluoride and silver nanoparticles on enamel demineralization and its antibiofilm activity against oral pathogens

Figure 1 - (A) TEM image of sodium trimetaphosphate decorated with silver nanoparticles (TMP-Ag); (B) Histogram of TEM image of Ag nanoparticles; (C) TEM images in a specific area of TMP-Ag nanoparticles; (D) EDS mapping in 2D presented a quantity of Potassium; (E) EDS mapping in 2D presented a dense quantity of silver distributed in the TMP-Ag nanoparticles.....49

Figure 2 – (A) TEM image of sodium trimetaphosphate (TMP) nanoparticles; (B) Histogram of TEM image of TMP nanoparticles and (C) Energy Dispersive Spectroscopy (EDS) of TMP nanoparticles.....50

Figure 3 - Profile of the hardness in longitudinal section (mean KHN, n = 12) as a function of the enamel depth according to the treatments. Values and comparisons between zones A and B are described in Table 1.....51

Figure 4 - Logarithm (mean \pm dp) of colony forming units normalized by adhesion area (\log_{10} CFU cm^{-2}) for *C. albicans* and *S. mutans* biofilms (single and mixed) after treatment for 24 h. Bars indicate SD of the mean. Different lowercase letters represent statistical difference between groups and concentrations tested (Fisher, $p < 0.001$). NC=negative control; PC=positive control (CHG); TMP=100F/TMP/Ag.....52

Figure 5 - SEM images of: *C. albicans* biofilms - (a) negative control, (b) positive control, (c) TMP 0,2%/F/Ag 10%; *S. mutans* biofilms - (d) negative control, (e) positive control, (f) TMP 0,2%/F/Ag 10%; mixed biofilms (*C. albicans* + *S. mutans*) – (g) negative control; (h) positive control; (i) TMP 0,2%/F/Ag 10%.....53

LISTA DE TABELAS

Capter 1: Sodium trimetaphosphate and hexametaphosphate impregnated with silver nanoparticles: characteristics and antimicrobial efficacy

Table 1 - MIC values of each composite and the controls tested against the two microorganisms.....23

Capter 2: *In vitro* evaluation of a composite containing sodium trimetaphosphate, fluoride and silver nanoparticles on enamel demineralization and its antibiofilm activity against oral pathogens

Table 1 - Mean values (SD) of percentage loss of surface hardness (% SH), integrated loss of subsurface hardness (Δ KHN) and chemical elements present in enamel according to treatments (n = 12).....48

SUMÁRIO

1. Introdução Geral.....	1
2. Capítulo 1 - Sodium trimetaphosphate and hexametaphosphate impregnated with silver nanoparticles: characteristics and antimicrobial efficacy	
2.1. Abstract.....	8
2.2. Introduction.....	8
2.3. Materials and methods.....	9
2.4. Results.....	13
2.5. Discussion.....	15
2.6. Conclusion.....	18
2.7. References.....	18
3 Capítulo 2 - <i>In vitro</i> evaluation of a composite containing sodium trimetaphosphate, fluoride and silver nanoparticles on enamel demineralization and its antibiofilm activity against oral pathogens	
3.1. Abstract.....	31
3.2. Introduction.....	32
3.3. Materials and methods.....	33
3.4. Results.....	38
3.5. Discussion.....	39
3.6. References.....	44

Introdução Geral

1. INTRODUÇÃO GERAL

A cárie dentária é considerada a doença mais prevalente nos seres humanos, atingindo 80-90% da população mundial [Petersen, 2004]. Sua etiologia já foi descrita como multifatorial por alguns autores [Keyes, 1960; Newbrune, 1978], enquanto outros defendiam ter um fator causador principal, como na revisão de Sheiham e James [Sheiham and James, 2015], na qual afirmam ser o açúcar o fator fundamental para o desenvolvimento desta doença. Mas o que é universalmente aceito é que a agressão à superfície dental é causada pela ação do *Streptococcus mutans* [Hamada and Slade, 1980] uma bactéria Gram ⁺, mais frequentemente encontrada no biofilme aderido à superfície do esmalte.

A patogenicidade do *S. mutans*, se dá primeiramente pela alta capacidade de formar biofilmes em superfícies sólidas [Huang et al., 2013; Shimotoyodome et al., 2007; Tamura et al., 2009]. O aumento da virulência das células de *S. mutans* ao formar biofilme também pode estar associado a uma maior tolerância ao baixo pH, em comparação com culturas planctônicas [Krzysciak et al., 2014]. No biofilme dental o *S. mutans* é um dos principais produtores de substâncias poliméricas extracelulares, os exopolissacarídeos (EPS). Uma matriz rica em EPS proporciona estabilidade e coesão mecânica ao biofilme e permite a criação de microambientes altamente ácidos, que são críticos para a patogênese da cárie dentária [Klein et al., 2015]. Contudo, o principal fator de virulência dessa bactéria é a secreção de ácidos [Banas, 2004], os quais levam à desmineralização do esmalte dentário e o aparecimento da lesão inicial de cárie.

Outros microrganismos também estão relacionados com a doença cárie, como a espécie fúngica *Candida albicans*, que apresenta importante papel como agente secundário, sendo responsável pela progressão do processo cariioso. De acordo com Pereira et al (2018) [Pereira et al., 2018], este fungo possui enzimas proteolíticas que contribuem para a colagenólise, evoluindo a doença particularmente para a cárie dentinária. Além disso, há indícios que a *C. albicans* tem a capacidade de aderir a hidroxiapatita por meio de interação eletrostática, e podendo levar a dissolução desse mineral [Nikawa et al., 2003].

O amplo espectro de ação contra microrganismos [Xiu et al., 2012] torna a prata um metal amplamente utilizado na prevenção da colonização de dispositivos médicos [Balazs et al., 2004; Monteiro et al., 2009], em curativos de feridas [Bjarnsholt et al., 2007; Gauger et al., 2003], em tratamentos de queimaduras [Khundkar et al., 2010; Ulkur et al., 2005]. Em sua forma nanoparticulada, a prata (AgNP) mostrou-se maior eficácia antimicrobiana por ser mais reativa [Panacek et al., 2006] e permitir uma maior área de contato e consequente interação com bactérias e fungos [Lok CN, 2006; Morones et al., 2005].

O flúor (F) foi o principal agente utilizado na prevenção da cárie dentária, podendo ser utilizado de forma sistêmica, nas águas de abastecimento público, ou de forma tópica como uso em dentifrícios, géis, enxaguatórios ou vernizes. O F tem uma ação importante ao manter o equilíbrio mineral dos dentes, agindo na dinâmica do processo de desmineralização e remineralização dentária [Ten Cate, 1990]. A descoberta das propriedades do F em relação à prevenção da cárie dentária pode ser considerada um marco na odontologia preventiva, e nesse sentido estudos vem sendo realizados visando melhorar a eficácia do F adicionando-o em produtos de higiene bucal e materiais restauradores provisórios.

McGaughey and Stowell (1977) [McGaughey and Stowell, 1977], divulgaram a eficiência de outros agentes, como os polifosfatos, capazes de modificar a superfície da hidroxiapatita através de sua adsorção, diminuindo a perda mineral e aumentando o processo de remineralização. Outros trabalhos reafirmaram que os fosfatos apresentam afinidade pelo esmalte reduzindo a perda mineral [da Camara et al., 2014; do Amaral et al., 2013; Takeshita et al., 2009]. A suplementação de dentifrícios com fosfatos inorgânicos e orgânicos e uma concentração reduzida de F aumentou o efeito anticárie desse produto [Danelon et al., 2014; do Amaral et al., 2013; Takeshita et al., 2009].

Dentre os polifosfatos, o trimetafosfato de sódio (TMP) tem sido testado com diferentes concentrações de F em vernizes, géis, enxaguatórios e dentifrícios e mostrou uma redução da perda mineral e aumentou o processo de remineralização, [Danelon et al., 2014; Favretto et al., 2013; Manarelli et al., 2011; Moretto et al., 2013]. Outro fosfato inorgânico, o hexametafosfato de sódio (HMP), é bem conceituado na indústria alimentícia como agente

antimicrobiano, devido sua capacidade de aumentar a permeabilidade da membrana externa bacteriana [Vaara and Jaakkola, 1989]. O HMP também apresenta habilidade de diminuir a solubilidade do esmalte [Van Dijk JW, 1980] e por isso estudos estão sendo conduzidos utilizando a associação HMP/F no tratamento anticárie em dentifrícios [da Camara et al., 2014].

Vale salientar que a utilização da proporção fosfato/fluoreto adequada é essencial para obter uma ação anticárie efetiva [Danelon et al., 2014; do Amaral et al., 2013; Favretto et al., 2013; Manarelli et al., 2013; Moretto et al., 2013; Takeshita et al., 2009]. Diante da grande ocorrência de cárie dentária e a crescente resistência microbiana frente à agentes antimicrobianos convencionais, o desenvolvimento de biomateriais capazes de inibir a desmineralização e induzir a remineralização da estrutura dentária, assim como apresentar atividade antibiofilme é de suma importância. No presente trabalho foram sintetizados nanocompósitos de Ag –TMP e –HMP e avaliou-se a efetividade contra biofilmes de *Candida albicans* e *Streptococcus mutans* e sua capacidade de inibição da desmineralização da superfície de esmalte dental bovino.

REFERÊNCIAS:

- Balazs DJ, Triandafillu K, Wood P, Chevolut Y, van Delden C, Harms H, Hollenstein C, Mathieu HJ: Inhibition of bacterial adhesion on pvc endotracheal tubes by rf-oxygen glow discharge, sodium hydroxide and silver nitrate treatments. *Biomaterials* 2004;25:2139-2151.
- Banas JA: Virulence properties of streptococcus mutans. *Frontiers in bioscience : a journal and virtual library* 2004;9:1267-1277.
- Bjarnsholt T, Kirketerp-Moller K, Kristiansen S, Phipps R, Nielsen AK, Jensen PO, Hoiby N, Givskov M: Silver against pseudomonas aeruginosa biofilms. *APMIS : acta pathologica, microbiologica, et immunologica Scandinavica* 2007;115:921-928.
- da Camara DM, Miyasaki ML, Danelon M, Sasaki KT, Delbem AC: Effect of low-fluoride toothpastes combined with hexametaphosphate on in vitro enamel demineralization. *Journal of dentistry* 2014;42:256-262.
- Danelon M, Takeshita EM, Peixoto LC, Sasaki KT, Delbem ACB: Effect of fluoride gels supplemented with sodium trimetaphosphate in reducing demineralization. *Clinical oral investigations* 2014;18:1119-1127.
- do Amaral JG, Sasaki KT, Martinhon CC, Delbem AC: Effect of low-fluoride dentifrices supplemented with calcium glycerophosphate on enamel demineralization in situ. *American journal of dentistry* 2013;26:75-80.
- Favretto CO, Danelon M, Castilho FC, Vieira AE, Delbem AC: In vitro evaluation of the effect of mouth rinse with trimetaphosphate on enamel demineralization. *Caries research* 2013;47:532-538.

- Gauger A, Mempel M, Schekatz A, Schafer T, Ring J, Abeck D: Silver-coated textiles reduce staphylococcus aureus colonization in patients with atopic eczema. *Dermatology* 2003;207:15-21.
- Hamada S, Slade HD: Biology, immunology, and cariogenicity of streptococcus mutans. *Microbiological reviews* 1980;44:331-384.
- Huang L, Xu QA, Liu C, Fan MW, Li YH: Anti-caries DNA vaccine-induced secretory immunoglobulin a antibodies inhibit formation of streptococcus mutans biofilms in vitro. *Acta pharmacologica Sinica* 2013;34:239-246.
- Keyes PH: The infectious and transmissible nature of experimental dental caries. Findings and implications. *Archives of oral biology* 1960;1:304-320.
- Khundkar R, Malic C, Burge T: Use of acticoat dressings in burns: What is the evidence? *Burns : journal of the International Society for Burn Injuries* 2010;36:751-758.
- Klein MI, Hwang G, Santos PH, Campanella OH, Koo H: Streptococcus mutans-derived extracellular matrix in cariogenic oral biofilms. *Frontiers in cellular and infection microbiology* 2015;5:10.
- Krzysciak W, Jurczak A, Koscielniak D, Bystrowska B, Skalniak A: The virulence of streptococcus mutans and the ability to form biofilms. *European journal of clinical microbiology & infectious diseases : official publication of the European Society of Clinical Microbiology* 2014;33:499-515.
- Lok CN HC, Chen R, He QY, Yu WY, Sun H, Tam PK, Chiu JF, Che CM: Proteomic analysis of the mode of antibacterial action of silver nanoparticles. *Journal of proteome research* 2006;5:9.
- Manarelli MM, Moretto MJ, Sasaki KT, Martinhon CC, Pessan JP, Delbem AC: Effect of fluoride varnish supplemented with sodium trimetaphosphate on enamel erosion and abrasion. *American journal of dentistry* 2013;26:307-312.
- Manarelli MM, Vieira AE, Matheus AA, Sasaki KT, Delbem AC: Effect of mouth rinses with fluoride and trimetaphosphate on enamel erosion: An in vitro study. *Caries research* 2011;45:506-509.
- McGaughey C, Stowell EC: Effects of polyphosphates on the solubility and mineralization of ha: Relevance to a rationale for anticaries activity. *Journal of dental research* 1977;56:579-587.
- Monteiro DR, Gorup LF, Takamiya AS, Ruvollo-Filho AC, de Camargo ER, Barbosa DB: The growing importance of materials that prevent microbial adhesion: Antimicrobial effect of medical devices containing silver. *International journal of antimicrobial agents* 2009;34:103-110.
- Moretto MJ, Delbem AC, Manarelli MM, Pessan JP, Martinhon CC: Effect of fluoride varnish supplemented with sodium trimetaphosphate on enamel erosion and abrasion: An in situ/ex vivo study. *Journal of dentistry* 2013;41:1302-1306.
- Morones JR, Elechiguerra JL, Camacho A, Holt K, Kouri JB, Ramirez JT, Yacaman MJ: The bactericidal effect of silver nanoparticles. *Nanotechnology* 2005;16:2346-2353.
- Newbrune E: *Cariology*. . Baltimore: Williams & Wilkins 1978:326.
- Nikawa H, Yamashiro H, Makihira S, Nishimura M, Egusa H, Furukawa M, Setijanto D, Hamada T: In vitro cariogenic potential of candida albicans. *Mycoses* 2003;46:471-478.
- Panacek A, Kvittek L, Pucek R, Kolar M, Vecerova R, Pizurova N, Sharma VK, Nevecna T, Zboril R: Silver colloid nanoparticles: Synthesis, characterization, and their antibacterial activity. *The journal of physical chemistry B* 2006;110:16248-16253.
- Pereira D, Seneviratne CJ, Koga-Ito CY, Samaranayake LP: Is the oral fungal pathogen candida albicans a cariogen? *Oral diseases* 2018;24:518-526.
- Petersen PE: Challenges to improvement of oral health in the 21st century--the approach of the who global oral health programme. *International dental journal* 2004;54:329-343.
- Sheiham A, James WP: Diet and dental caries: The pivotal role of free sugars reemphasized. *Journal of dental research* 2015;94:1341-1347.

- Shimotoyodome A, Kobayashi H, Tokimitsu I, Hase T, Inoue T, Matsukubo T, Takaesu Y: Saliva-promoted adhesion of streptococcus mutans mt8148 associates with dental plaque and caries experience. *Caries research* 2007;41:212-218.
- Takeshita EM, Castro LP, Sasaki KT, Delbem AC: In vitro evaluation of dentifrice with low fluoride content supplemented with trimetaphosphate. *Caries research* 2009;43:50-56.
- Tamura S, Yonezawa H, Motegi M, Nakao R, Yoneda S, Watanabe H, Yamazaki T, Senpuku H: Inhibiting effects of streptococcus salivarius on competence-stimulating peptide-dependent biofilm formation by streptococcus mutans. *Oral microbiology and immunology* 2009;24:152-161.
- Ten Cate JM: In vitro studies on the effects of fluoride on de- and remineralization. *Journal of dental research* 1990;69 Spec No:614-619; discussion 634-616.
- Ulkur E, Oncul O, Karagoz H, Yeniz E, Celikoz B: Comparison of silver-coated dressing (acticoat), chlorhexidine acetate 0.5% (bactigrass), and fusidic acid 2% (fucidin) for topical antibacterial effect in methicillin-resistant staphylococci-contaminated, full-skin thickness rat burn wounds. *Burns : journal of the International Society for Burn Injuries* 2005;31:874-877.
- Vaara M, Jaakkola J: Sodium hexametaphosphate sensitizes pseudomonas aeruginosa, several other species of pseudomonas, and escherichia coli to hydrophobic drugs. *Antimicrobial agents and chemotherapy* 1989;33:1741-1747.
- Van Dijk JW BJ, Driessens FC: The effect of some phosphates and a phosphonate on the electrochemical properties of bovine enamel. *Archives of oral biology* 1980; 25.
- Xiu ZM, Zhang QB, Puppala HL, Colvin VL, Alvarez PJ: Negligible particle-specific antibacterial activity of silver nanoparticles. *Nano letters* 2012;12:4271-4275.
- .

Capítulo 1

Sodium trimetaphosphate and hexametaphosphate impregnated with silver nanoparticles: characteristics and antimicrobial efficacy

**Artigo publicado no periódico Biofouling*

Sodium trimetaphosphate and hexametaphosphate impregnated with silver nanoparticles: characteristics and antimicrobial efficacy.

ABSTRACT

This study aimed to synthesize and characterize materials containing silver nanoparticles (AgNP) with polyphosphates (sodium trimetaphosphate (TMP) or sodium hexametaphosphate (HMP)), and evaluate their effect against *Candida albicans* and *Streptococcus mutans*. The minimum inhibitory concentration (MIC) was determined, which was followed by the quantification of the biofilm by counting colony-forming units (CFUs), the amount of metabolic activity, and the total biomass. The MICs revealed greater effectiveness of composites containing 10% Ag (TMP + Ag10% (T10) and HMP + Ag10% (H10)) against both microorganisms. It was observed that T10 and H10 reduced the formation of biofilms by 56–76% for *C. albicans* and by 52–94% for *S. mutans* for total biomass and metabolic activity. These composites promoted significant log reductions in the number of CFUs, between 0.45–1.43 log₁₀ for *C. albicans* and 2.88–3.71 log₁₀ for *S. mutans* ($p < .001$). These composites demonstrated significant antimicrobial activity, especially against *S. mutans*, and may be considered a potential alternative for new dental materials.

INTRODUCTION

Streptococcus mutans is the main cariogenic microorganism, and its capacity to produce acid and survive at low pH, as well as its ability to synthesize extracellular polysaccharides, are important virulence factors which contribute to the colonization of the tooth surface, development of pathogenic biofilms, and enamel demineralization (Leone et al. 2008, Li and Chang 2008; Delbem et al. 2014). Although the development of dental caries is related to the formation of biofilm, the progression of established lesions may include species of *Candida*, particularly *Candida albicans* (Shibata and Morioka 1982; Monteiro et al. 2015).

Composites containing calcium and phosphate have shown promising anticariostatic effects (do Amaral et al. 2013; Takeshita et al. 2015; da Camara et al. 2016). Among the phosphate salts, sodium trimetaphosphate (TMP) and sodium hexametaphosphate (HMP) have been effective in reducing enamel demineralization and improving remineralization. They are inorganic

cyclophosphates with the capacity to adsorb hydroxyapatite and protein through hydroxyl (Souza et al. 2013; Delbem et al. 2014) and amino (Leone et al. 2008; Li and Chang 2008) attachment sites. Added to low concentrations of fluoride in an appropriate proportion in oral health products, they provide a greater protective effect than conventional fluoride products (da Camara et al. 2014; Manarelli et al. 2015; Takeshita et al. 2015; Conceicao et al. 2015; da Camara et al. 2016).

The development of multifunctional biomaterials to be used in the health field is the focus of increasing attention. Added to that, the exponential growth of nanotechnology, and the use of silver nanoparticles (AgNP) as an antimicrobial agent allowing for increased surface-to-volume ratios and specific interactions with species of bacteria and fungi (Baker et al. 2005, Morones et al. 2005; Lok et al. 2006), new approaches could be useful to prevent and control dental caries. A material containing AgNP as an antimicrobial agent, and sources of fluoride and phosphate to prevent the demineralization of dental enamel could achieve promising results. Thus, this study aimed to synthesize composites containing AgNP, F, and TMP or HMP, and to characterize and evaluate their effect against *Streptococcus mutans* and *Candida albicans*.

MATERIALS AND METHODS

Synthesis and characterization of the nanocomposites

Nanocomposites were synthesized based on the protocol proposed by Miranda et al. (2010), with some modifications. The synthesis was carried out in an alcoholic medium (isopropanol) using sodium borohydride (NaBH_4 , Sigma-Aldrich, St Louis, MO, USA) as a reducing agent. Suspensions containing sodium trimetaphosphate (TMP, Sigma-Aldrich, CAS 7785-84-4) or sodium hexametaphosphate (HMP, Sigma-Aldrich, CAS 68915-31-1), fluoride (NaF , Merck, Darmstadt, Germany), and silver nitrate (AgNO_3 , Merck) were prepared in the presence of a surfactant (ammonium salt of polymethacrylic acid (NHPM), Polysciences, Inc., Warrington, PA, USA). AgNO_3 was employed at 1% or 10% of the phosphate weight. The molar proportions between phosphates and fluoride was 1.2:1 TMP/ NaF or 0.62:1 HMP/ NaF , and between silver ions (Ag^+) and NaBH_4 it was 1:1.26. Samples were dried overnight at 70°C. AgNP with no polyphosphates was also synthesized.

The morphology of the nanocomposites was characterized by scanning electron microscopy (SEM) on a Zeiss Supra 35VP microscope (S-360 microscope, Leo, MA, USA) with field emission gun electron effect (FEG-SEM, 10 kV). A drop of each sample was placed on a silicon substratum and dried at 40°C for 12 h. Two-dimensional images were constructed by analyzing the P K α , Ag L α 1, and O K α energy emissions using energy dispersive X-ray detector (EDX) analysis with mapping. Samples were also characterized by X-ray diffraction (XRD) (Rigaku diffractometer [Rigaku Corporation, Tokyo, Japan], DMax 2500PC) with CuK radiation ($\lambda = 1.5406$ Å) generated at a voltage of 40 kV and a current of 40 mA. The scanning range (2θ) was from 20° to 110° with a step size of 0.2°, a 1.0 mm divergent slit, 0.2 mm collection slot, and accumulation for reading every 0.02 s.

Determination of Ag⁺ concentration

The concentration of Ag⁺ in the composites was determined by a 9616 BNWP (Thermo Scientific, Beverly, MA, USA) ion-specific electrode coupled to an ion analyzer (Orion 720 A⁺, Thermo Scientific). One thousand $\mu\text{g Ag ml}^{-1}$ were prepared (1.57 g of dried AgNO₃ for 1 l of deionized water) as a standard, and diluted in deionized water to achieve equivalent silver concentrations in the composites. Thus, the combined electrode was calibrated with solutions containing 6.25 to 100 $\mu\text{g Ag ml}^{-1}$. A silver ionic strength adjuster solution (ISA, Cat. No. 940011), which provides a constant background ionic strength was used (1 ml of each sample/standard: 0.02 ml of ISA).

Minimum inhibitory concentration (MIC)

The microdilution method was performed following the Clinical Laboratory Standards Institute guidelines (CLSI: M27-A2 and M07-A9). The nanocomposites were diluted in deionized water in geometric progression, from 2 to 1,024 times. Afterwards, each nanocomposite concentration obtained previously was diluted (1:5) in RPMI 1640 medium (Sigma-Aldrich) for *Candida albicans* (ATCC 10231), and in brain heart infusion (BHI, Difco, Le Pont de Claix, France) for *Streptococcus mutans* (ATCC 25175). Inocula from 24-h cultures were adjusted to the 0.5 McFarland standard turbidity equivalent in saline solution (0.85% NaCl). Suspensions of each strain were diluted (1:5) in

saline and subsequently diluted (1:20) in RPMI 1640 for *C. albicans* or BHI broth for *S. mutans*. Each microorganism suspension (100 μ l) was added in the wells of microtiter plates containing 100 μ l of each nanocomposite concentration. Polyphosphate/fluoride, AgNP, and chlorhexidine gluconate (CHG) (Periogard-Colgate, New York, NY, USA) were tested as controls. The microtiter plates were incubated at 37°C, and the MICs were determined visually as the lowest concentration of nanocomposites with no microorganism growth after 48 h.

Biofilm formation and treatment

Single species biofilms were grown in 96-well microtiter plates (Costar, Corning Incorporated, Tewksbury, MA, USA) containing 0.2 ml of *C. albicans* cell suspension (1×10^7 cells ml^{-1} in artificial saliva) (Silva et al. 2010) or 0.2 ml of *S. mutans* (1×10^8 cells ml^{-1} in artificial saliva) (Arias et al. 2016). The plates were incubated at 37°C for 24 h. After this period, the biofilm-containing wells were washed with 0.2 ml of phosphate buffered saline (PBS; pH 7, 0.1 M) to remove the non-adherent cells. Next, the nanocomposites were added to the biofilms at concentrations based on the MIC values obtained previously. For this, 0.2 ml of the T10 and H10 nanocomposites at MIC and $10 \times$ MIC were diluted in artificial saliva, which was added to the biofilm-containing wells. AgNP with no phosphates and CHG at 0.018% (positive control) were also tested against the biofilms, and artificial saliva with no nanocomposites was used as negative control. The biofilms were then re-incubated at 37°C for 24 h.

Biofilm quantification

The quantification of *C. albicans* and *S. mutans* cultivable cells from biofilms treated with T10 and H10 was carried out by counting colony-forming units (CFUs). For this, the biofilm-containing wells were scraped with a tip, using 0.2 ml of PBS each time five times, totaling 1 ml of suspension, and the cell suspensions were then placed in Falcon tubes. The suspensions were vortexed and serially diluted in PBS and plated on SDA (*C. albicans*) or BHI (*S. mutans*).

After incubation at 37°C for 24 h for *C. albicans* and 48 h for *S. mutans*, the total number of CFUs was counted and the log CFU per unit area (\log_{10}

CFU cm^{-2}) was determined. After the biofilms were treated, the total biomass was analyzed by the crystal violet (CV) method (Monteiro et al. 2015). The biofilms were washed with 0.2 ml of PBS and fixed by adding 0.2 ml of 99% methanol (Sigma-Aldrich) for 15 min. The methanol was then removed and the wells were allowed to dry at room temperature. Then, 0.2 ml of CV (1%, v v^{-1} , Merck) were added into each well, and after 5 min, the excess was withdrawn by washing each well-plate with deionized water. CV bound to the biofilms was eluted using 0.2 ml of acetic acid (33%, v v^{-1} , Sigma-Aldrich), and the absorbance was measured in a microtiter-plate reader (Eon Microplate Spectrophotometer; Bio Tek, Winooski, VT, USA) at 570 nm, and standardized in relation to the area of the well-plate (Abs 570 nm cm^{-2}).

Metabolic activity was assessed by the XTT reduction assay (2,3-bis (2-methoxy-4-nitro-5-sulfophenyl)-5-[(phenylamino)carbonyl]-2H-tetrazolium hydroxide (Sigma-Aldrich). Biofilm-containing wells were washed once with 0.2 ml of PBS and 0.2 ml of the solution containing 150 mg XTT l^{-1} and 10 mg of phenazine methosulfate l^{-1} in each well. The plates were then incubated at 37°C, under agitation at 120 rpm, in the dark. After 3 h, the absorbance was read at 490 nm cm^{-2} . All assays were performed, independently and in triplicate, on three different occasions.

Microscopy

The structural analysis of single biofilms of *C. albicans* and *S. mutans* exposed to the nanocomposites was verified by SEM. Briefly, the biofilms were formed in 24-well plates as described before. Then, the T10 and H10 nanocomposites were added to the wells at the concentration of 10/100 $\mu\text{g Ag ml}^{-1}$ for *C. albicans* and 40/400 $\mu\text{g Ag ml}^{-1}$ for *S. mutans* biofilms. After treatment for 24 h, the wells were washed with PBS and the biofilms were dehydrated using an ethanol concentration series (70% for 10 min, 95% for 10 min, and 100% for 20 min), followed by air drying for 20 min (Silva et al. 2013). The bottom of the wells were cut with a scalpel blade (number 11, Solidor, Lamedid Commercial and Services Ltda, Barueri, Brazil) heated in flame, and the biofilms were coated with gold for scanning with the electron microscope (S-360 microscope, Leo, Cambridge, MA, USA) (Fernandes et al. 2016).

Statistical analysis

SigmaPlot 12.0 software (Systat Software Inc., San Jose, CA, USA) was used for statistical analysis; the significance level was set at 5%. CFUs, CV (for both microorganisms tested), and XTT (*C. albicans*) data exhibited a normal and homogeneous distribution (Shapiro–Wilks test) and were submitted to one-way analysis of variance, followed by the Fisher test. XTT data from *S. mutans* were submitted to logarithmic transformation and one-way analysis of variance followed by the Fisher test.

RESULTS

Synthesis, characterization, and Ag⁺ determination in the nanocomposites

XRD and SEM demonstrated the association of silver nanoparticles in both polyphosphates (sodium trimetaphosphate (TMP) and sodium hexametaphosphate (HMP)). The typical XRD pattern of the prepared T1 (TMP+Ag1%) and T10 (TMP+Ag10%) powder showed diffraction peaks at $2\theta = 14.4^\circ$, 17.3° , 23.4° , 26.1° , and 29.2° , and the corresponding crystallographic form (PDF № 72–1628) of the TMP salt (Figure 1a). Figure 1a shows diffraction peaks at $2\theta = 38.2^\circ$, 44.4° , and 64.6° , which can be indexed to (2 0 0), (1 1 1), and (2 2 0) planes of pure silver with the face centered cubic system (PDF № 04–0783). Figure 1b shows the X-ray diffraction patterns of HMP that present a wide halo between 15° and 35° , characteristic of amorphous materials. The X-ray diffraction patterns of H1 (HMP+Ag1%) and H10 (HMP+Ag10%) indicate sodium hexametaphosphate salt – $(\text{NaPO}_3)_6$ (PDF № 3643), and suggest the presence of other polyphosphate salts, such as $(\text{NaH}_2\text{PO}_4 \cdot \text{H}_2\text{O})$, NaH_2PO_4 , $\text{Na}_5\text{P}_3\text{O}_{10}$, NaPO_3 , and $\text{Na}_2\text{H}_2\text{P}_2\text{O}_7$, by comparing the experimentally obtained XRD patterns with standard patterns (PDF № 11–651, 11–659, 11–652, 76–788, and 11–657). SEM images of T10 and H10 (Figure 2) show silver nanoparticles (white shades) dispersed and decorating the surface of the phosphates at micrometric size (gray shades). AgNP anchored on the surface of HMP or TMP were more evident in samples containing Ag at 10% than at 1% of Ag. The 2-D images were constructed by analyzing the energy released from the O K α , P K α (constituents of the TMP and HMP material) and Ag K α

emissions, indicating the uniform distribution of these elements in the demarcated area in the micrograph.

The total amount of Ag^+ (from the AgNO_3 source) added to the reaction to obtain AgNP with no TMP or HMP was $20,000 \mu\text{g Ag ml}^{-1}$, and the ionic concentration was determined by electrode method at $576.19 \mu\text{g Ag ml}^{-1}$, thus a reduction of 97.12% of ionic silver was observed. All samples containing Ag at 1% (H1 and T1) or 10% (H10 and T10) presented Ag^+ % reduction between 98.04 and 99.85%. For H1 and T1 samples, the Ag concentrations were determined as 1.43 and $8.13 \mu\text{g Ag}^+ \text{ml}^{-1}$, and the total amount of Ag used in the reaction was $1,000 \mu\text{g Ag ml}^{-1}$. For H10 and T10 samples, the Ag concentrations were 129.8 and $195.4 \mu\text{g Ag}^+ \text{ml}^{-1}$, and the total amount of Ag used in the reaction was $10,000 \mu\text{g Ag ml}^{-1}$.

Antimicrobial effect

The nanocomposites were effective against both strains tested in planktonic form (Table 1). Composites containing Ag at 10% (T10 and H10) were more effective against *C. albicans* ($10 \mu\text{g Ag V}$) than against *S. mutans* ($40 \mu\text{g Ag V}$), while at 1% Ag only H1 presented an effect against the microorganisms ($80 \mu\text{g Ag V}$). For the group of AgNP without TMP or HMP synthesized in the same conditions, the MIC values were $62.5 \mu\text{g Ag ml}^{-1}$ for *C. albicans* and $125 \mu\text{g Ag ml}^{-1}$ for *S. mutans*. At lower Ag concentration (1%), only H1 presented an antimicrobial effect. In this study, biofilm cells of *C. albicans* were resistant to all concentrations tested of AgNP without phosphates (Figure 3). However, after adding the polyphosphates to the AgNP, there were significant reductions of $1.43 \log_{10}$ in the *C. albicans* biofilm treated with T10, and $1.17 \log_{10}$ treated with H10 ($100 \mu\text{g Ag ml}^{-1}$) (Figure 3a), when compared to the negative control group ($p = 0.004$ and $p = 0.014$). Surprisingly, *S. mutans* biofilm cells were more susceptible to T10 and H10 than the *C. albicans* biofilm cells, and they were similar to the CHG positive control (PC) (Figure 3a). Notably, there was a reduction of $4.2 \log_{10}$ in the *S. mutans* biofilm at the lowest concentration ($40 \mu\text{g Ag ml}^{-1}$) of T10.

The total biomass quantification and metabolic activity in the *C. albicans* and *S. mutans* biofilms are shown in Figure 3b and c. Significant reductions (~75%) in the total biomass of both microorganisms were observed in the lowest

concentrations of T10 ($10 \mu\text{g Ag ml}^{-1}$) and H10 ($40 \mu\text{g Ag ml}^{-1}$), being similar to CHG (PC) (Figure 3b). Notably, the metabolic activity (Figure 3c) of *C. albicans* biofilm was reduced (93.4–94.4%) at both 10 and $100 \mu\text{g Ag ml}^{-1}$ of T10 and at $100 \mu\text{g Ag ml}^{-1}$ of H10 (92.0%). T10 and H10 nanocomposites reduced the metabolic activity of *S. mutans* biofilms by ~ 90%, at all concentrations tested.

Microscopy

Figure 4 shows hyphal cell density similar to the negative control in all *C. albicans* biofilms exposed to nanocomposites T10 and H10, while a reduction in cellular biomass was observed in biofilm treated with chlorhexidine gluconate. On the other hand, the quantity of cells in the *S. mutans* biofilms treated with T10 and H10 was as suppressed as in the biofilm subjected to chlorhexidine gluconate treatment (Figure 5).

DISCUSSION

This study evaluated the antimicrobial action of nanocomposites against strains of *C. albicans* and *S. mutans* in both the planktonic form and in biofilms grown for 24 h. Analyses included the quantification of viable cells, total biomass, and metabolic activity.

Currently, there are several studies in the literature that show the mechanism of action of silver nanoparticles. As has already been demonstrated, silver nanoparticles promote direct damage to the cellular membrane by adhering to it (Li et al. 2008) or by dissolving it through the release of silver ions (Kon and Rai 2013). Then, once inside the cell of the microorganism, silver nanoparticles can lead to DNA damage (Li et al. 2008), mainly *via* production of ROS (Marambio-Jones and Hoek 2010; Duran et al. 2016), and can also affect the electrochemical proton gradient through the respiratory process, which could discontinue the ATP synthesis, leading to the death of the microorganism cell (Reidy et al. 2013).

The combination of silver nanoparticles with other compounds may improve their antimicrobial activity (Pal et al. 2007; Monteiro et al. 2013). The results of the present study demonstrated that the association of AgNP with TMP or HMP did not hinder the antimicrobial silver effect, but the association of Ag and polyphosphates resulted in similar MICs at a lower Ag concentration

(Table 1). The crystallographic surface structures of AgNP are an important physico-chemical property which is related to their antibacterial activity (Pal et al. 2007), and could be changed when associated with those polyphosphates. The composites were more effective against planktonic cells of *C. albicans* ($10 \mu\text{g Ag ml}^{-1}$) than *S. mutans* (40 Ag ml^{-1}) when the Ag concentration was 10% (T10 and H10), while at 1%, just H1 showed an antimicrobial effect ($80 \mu\text{g Ag ml}^{-1}$). HMP has the ability to increase outer membrane cell permeability (Shibata and Morioka 1982; Vaara and Jaakkola 1989), and it might facilitate Ag entrance into the microorganism cells. Indeed, the polyphosphate property of adsorption on protein by hydroxyl and amino sites (Leone et al. 2008; Li and Chang 2008) may increase Ag availability and improve the antimicrobial effect of those composites. This was observed especially for T10 (TMP+Ag10%) and H10, (HMP+Ag10%) which have a higher Ag concentration impregnated on the phosphates. H1 (HMP+Ag1%) alone was shown to be effective against both planktonic strains. These results demonstrate that not only was the amount of Ag relevant for the antimicrobial effectiveness of the composites, but its association with the phosphates had a significant role in the increase in the antimicrobial potential of the TMP/HMP-AgNP nanocomposites. This has also been demonstrated by Humphreys et al. (2011) and the synergism between polyphosphates and silver might increase the permeability of the outer membrane of bacteria associated to sequestration of divalent cations by polyphosphate (Maier et al. 1999; Akhtar et al. 2008; Obritsch et al. 2008), enabling silver to pass through the membrane and then causing damage to the cell, such as loss of DNA replication and protein inactivation (Feng et al. 2000).

The greater susceptibility of planktonic cells of *C. albicans* in comparison to *S. mutans* planktonic cells can be primarily explained by the structural differences in their cell membranes (Malanovic and Lohner 2016). Membranes of bacteria are negatively charged due to anionic phospholipids, while the charge in fungal membranes is neutral, constituted by zwitterionic phospholipids and ergosterol. The work of Abbaszadegan et al. (2015) states that the antimicrobial action of the nanoparticle shell depends on the charge of the external surface of the particles as influenced by the stabilizers and capping agents used in the synthesis; thus, the AgNP fabricated in the present study can be considered negatively charged. According to Mandal et al. (2016), the

mechanism of AgNP action depends on the outer charge of the bacterial membranes, and this may explain the decreased susceptibility of *S. mutans*. Furthermore, the physical and chemical properties of the AgNP related to the release of Ag⁺ ions are noteworthy. It seemed that AgNP were more clearly adhered to the surface of TMP than the surface of HPM (Figure 2a and c). This could facilitate the release of Ag⁺ ions, and hence, its highest concentration in the composites containing TMP, regardless of the amount of AgNO₃ (1 or 10%) used in the synthesis reaction. On the other hand, it did not increase the antimicrobial effectiveness of the T10, suggesting antimicrobial activity is not just related to the amount of Ag⁺ ions released from that composite.

However, many antimicrobial agents that show effectiveness against planktonic cells could be ineffective against the same microorganism grown in a biofilm (Jefferson 2004; Kim et al. 2008). Biofilms of *Candida* species, for example, can exhibit up to 65 times more tolerance to killing by metals than corresponding planktonic cultures (Harrison et al. 2007). Although biofilms of *C. albicans* showed tolerance against pure AgNP (Figure 3a), the addition of the polyphosphates resulted in inhibition of the growth of fungal biofilms. The same occurred against biofilm cells of *S. mutans*. Nevertheless, the microscopy images (Figures 4 and 5) show that growth of *C. albicans* biofilm cells was similar to the negative control, while the reduction in biofilm cells of *S. mutans* was consistent with chlorhexidine gluconate, as shown through CFU analysis. The explanation would also be related to the mechanism of action of polyphosphates on planktonic cells (Maier et al. 1999; Akhtar et al. 2008; Obritsch et al. 2008), and also for a probable buffer effect promoted by the phosphates in the *S. mutans* biofilm environment. To this end, as *S. mutans* is an acidogenic and aciduric bacterial strain, TMP and HMP may have hampered the decrease in pH, and hence, the proliferation of the cells in the biofilm.

The total biomass and metabolic activity of fungal and bacterial biofilms are shown in Figure 3b and c. Overall, the methods used to quantify microbial biofilms were performed as complementary analysis. As shown in the results, the lowest concentrations of T10 (10 µg Ag ml⁻¹) and H10 (40 µg Ag ml⁻¹) were able to reduce the total biomass in a manner similar to the positive control (CHG). Figure 3c shows the reduction in biofilm activity of *C. albicans* of between 92 and 94.4%, with the exception of the concentration of 10 µg Ag ml⁻¹

H10. All concentrations of both T10 and H10 reduced the biofilm biomass of *S. mutans* by ~ 90%. Nevertheless, it is noteworthy that *S. mutans* may not have properly absorbed and/or metabolized the salt of XTT (Kuhn et al. 2003; Gobor et al. 2011), and hence, interfered with the spectrophotometer reading since there was also low metabolic activity in the negative control group (NC).

Finally, looking at the antimicrobial effect of the polyphosphates TMP or HMP-AgNP in comparison with AgNP alone, the findings of the present study demonstrate that both TMP and HMP with a very low NaF concentration substantially improved the effectiveness of AgNP against both the planktonic and sessile forms of the microorganism. This suggests that AgNP associated with TMP or HMP polyphosphates and fluoride may be effective antimicrobial biomaterials for promising applications to control caries disease. Future studies should investigate the remineralization potential of these composites as well as their toxicity to make their incorporation in dental materials feasible. Studies considering different approaches to investigate the mechanisms of action of these nanocomposites would also be opportune.

CONCLUSION

In this study, nanocomposites formed by AgNP associated with TMP or HMP polyphosphates and very low concentrations of fluoride were synthesized. The antimicrobial and anti-biofilm effectiveness of these nanocomposites were observed against *S. mutans* and *C. albicans*, both relevant dental caries pathogens. Furthermore, the results suggest that TMP and HMP improved the antimicrobial potential of AgNP, enabling the use of smaller amounts of AgNP to produce more biocompatible nanomaterials, which would be effective at reducing caries –inducing pathogens and increasing the dental remineralization process.

REFERENCES

- Abbaszadegan A, Ghahramani Y, Gholami A, Hemmateenejad B, Dorostkar S, Nabavizadeh M, Sharghi H. 2015. The effect of charge at the surface of silver nanoparticles on antimicrobial activity against gram-positive and gram-negative bacteria: a preliminary study. *J Nanomater.* 2015:1–8.

- Akhtar S, Paredes-Sabja D, Sarker MR. 2008. Inhibitory effects of polyphosphates on *Clostridium perfringens* growth, sporulation and spore outgrowth. *Food Microbiol.* 25:802–808. doi:10.1016/j.fm.2008.04.006
- do Amaral, JG, Sasaki KT, Martinhon CC, Delbem AC. 2013. Effect of low-fluoride dentifrices supplemented with calcium glycerophosphate on enamel demineralization *in situ*. *Am J Dent.* 26:75–80.
- Arias LS, Delbem AC, Fernandes RA, Barbosa DB, Monteiro DR. 2016. Activity of tyrosol against single and mixed-species oral biofilms. *J Appl Microbiol.* 120:1240–1249. doi:10.1111/jam.2016.120.issue-5
- Baker C, Pradhan A, Pakstis L, Pochan DJ, Shah SI. 2005. Synthesis and antibacterial properties of silver nanoparticles. *J Nanosci Nanotechnol.* 5:244–249.
- da Camara DM, Miyasaki ML, Danelon M, Sasaki KT, Delbem AC. 2014. Effect of low-fluoride toothpastes combined with hexametaphosphate on *in vitro* enamel demineralization. *J Dent.* 42:256–262. doi:10.1016/j.jdent.2013.12.002
- da Camara DM, Pessan JP, Francati TM, Souza JA, Danelon M, Delbem AC. 2016. Fluoride toothpaste supplemented with sodium hexametaphosphate reduces enamel demineralization *in vitro*. *Clin Oral Investig.* 20:1981–1985. doi:10.1007/s00784-015-1707-x
- Conceicao JM, Delbem AC, Danelon M, da Camara DM, Wiegand A, Pessan JP. 2015. Fluoride gel supplemented with sodium hexametaphosphate reduces enamel erosive wear *in situ*. *J Dent.* 43:1255–1260. doi:10.1016/j.jdent.2015.08.006
- Delbem AC, Souza JA, Zaze AC, Takeshita EM, Sasaki KT, Moraes JC. 2014. Effect of trimetaphosphate and fluoride association on hydroxyapatite dissolution and precipitation *in vitro*. *Braz Dent J.* 25:479–484. doi:10.1590/0103-6440201300174
- Duran N, Duran M, de Jesus MB, Seabra AB, Favaro WJ, Nakazato G. 2016. Silver nanoparticles: a new view on mechanistic aspects on antimicrobial activity. *Nanomedicine.* 12:789–799. doi:10.1016/j.nano.2015.11.016
- Feng QL, Wu J, Chen GQ, Cui FZ, Kim TN, Kim JO. 2000. A mechanistic study of the antibacterial effect of silver ions on *Escherichia coli* and *Staphylococcus aureus*. *J Biomed Mater Res.* 52:662–668. doi:10.1002/(ISSN)1097-4636
- Fernandes RA, Monteiro DR, Arias LS, Fernandes GL, Delbem AC, Barbosa DB. 2016. Biofilm formation by *Candida albicans* and *Streptococcus mutans* in the presence of farnesol: a quantitative evaluation. *Biofouling.* 32:329–338. doi:10.1080/08927014.2016.1144053
- Gobor T, Corol G, Ferreira LE, Rymovicz AU, Rosa RT, Campelo PM, Rosa EA. 2011. Proposal of protocols using D-glutamine to optimize the 2,3-bis(2-methoxy-4-nitro-5-sulfophenyl)-5-[(phenylamino)carbonyl]-2H-tetrazolium hydroxide (XTT) assay for indirect estimation of microbial loads in biofilms of medical importance. *J Microbiol Methods.* 84:299–306. doi:10.1016/j.mimet.2010.12.018

- Harrison JJ, Ceri H, Yerly J, Rabiei M, Hu Y, Martinuzzi R, Turner RJ. 2007. Metal ions may suppress or enhance cellular differentiation in *Candida albicans* and *Candida tropicalis* biofilms. *Appl Environ Microbiol.* 73:4940–4949. doi:10.1128/AEM.02711-06
- Humphreys G, Lee GL, Percival SL, McBain AJ. 2011. Combinatorial activities of ionic silver and sodium hexametaphosphate against microorganisms associated with chronic wounds. *J Antimicrob Chemother.* 66:2556–2561. doi:10.1093/jac/dkr350
- Jefferson KK. 2004. What drives bacteria to produce a biofilm? *FEMS Microbiol Lett.* 236:163–173. doi:10.1111/fml.2004.236.issue-2
- Kim J, Pitts B, Stewart PS, Camper A, Yoon J. 2008. Comparison of the antimicrobial effects of chlorine, silver ion, and tobramycin on biofilm. *Antimicrob Agents Chemother.* 52:1446–1453. doi:10.1128/AAC.00054-07
- Kon K, Rai M. 2013. Metallic nanoparticles: mechanism of antibacterial action and influencing factors. *J Comp Clin Pathol Res.* 1:160–174.
- Kuhn DM, Balkis M, Chandra J, Mukherjee PK, Ghannoum MA. 2003. Uses and limitations of the XTT assay in studies of *Candida* growth and metabolism. *J Clin Microbiol.* 41:506–508. doi:10.1128/JCM.41.1.506-508.2003
- Leone G, Torricelli P, Giardino R, Barbucci R. 2008. New phosphorylated derivatives of carboxymethylcellulose with osteogenic activity. *Polym Adv Technol.* 19:824–830.
- Li X, Chang J. 2008. Preparation of bone-like apatite/collagen nanocomposites by a biomimetic process with phosphorylated collagen. *J Biomed Mater Res A.* 85:293–300. doi:10.1002/(ISSN)1552-4965
- Li Q, Mahendra S, Lyon DY, Brunet L, Liga MV, Li D, Alvarez PJ. 2008. Antimicrobial nanomaterials for water disinfection and microbial control: potential applications and implications. *Water Res.* 42:4591–4602. doi:10.1016/j.watres.2008.08.015
- Lok CN, Ho CM, Chen R, He QY, Yu WY, Sun H, Tam PK, Chiu JF, Che CM. 2006. Proteomic analysis of the mode of antibacterial action of silver nanoparticles. *J Proteome Res.* 5:916–924.
- Maier SK, Scherer S, Loessner MJ. 1999. Long-chain polyphosphate causes cell lysis and inhibits *Bacillus cereus* septum formation, which is dependent on divalent cations. *Appl Environ Microbiol.* 65:3942–3949.
- Malanovic N, Lohner K. 2016. Gram-positive bacterial cell envelopes: the impact on the activity of antimicrobial peptides. *Biochim Biophys Acta.* 1858:936–946. doi:10.1016/j.bbamem.2015.11.004
- Manarelli MM, Delbem AC, Binhardi TD, Pessan JP. 2015. In situ remineralizing effect of fluoride varnishes containing sodium trimetaphosphate. *Clin Oral Investig.* 19:2141–2146. doi:10.1007/s00784-015-1492-6
- Mandal D, Kumar Dash S, Das B, Chattopadhyay S, Ghosh T, Das D, Roy S. 2016. Bio-fabricated silver nanoparticles preferentially targets Gram positive depending on cell surface charge. *Biomed Pharmacother.* 83:548–558. doi:10.1016/j.biopha.2016.07.011

- Marambio-Jones C, Hoek E. 2010. A review of the antibacterial effects of silver nanomaterials and potential implications for human health and the environment. *J Nanopart Res.*12:1531–1551. doi:10.1007/s11051-010-9900-y
- Miranda M, Fernandez A, Diaz M, Esteban-Tejeda L, Lopez-Esteban S, Malpartida F, Torrecillas R, Moya JS. 2010. Silver-hydroxyapatite nanocomposites as bactericidal and fungicidal materials. *Int J Mater Res.* 101:122–127.
- Monteiro DR, Feresin LP, Arias LS, Barao VA, Barbosa DB, Delbem AC. 2015. Effect of tyrosol on adhesion of *Candida albicans* and *Candida glabrata* to acrylic surfaces. *Med Mycol.* 53:656–665. doi:10.1093/mmy/myv052
- Monteiro DR, Silva S, Negri M, Gorup LF, de Camargo ER, Oliveira R, Barbosa DB, Henriques M. 2013. Antifungal activity of silver nanoparticles in combination with nystatin and chlorhexidine digluconate against *Candida albicans* and *Candida glabrata* biofilms. *Mycoses.* 5:672–680. doi:10.1111/ myc.2013.56.issue-6
- Morones JR, Elechiguerra JL, Camacho A, Holt K, Kouri JB, Ramirez JT, Yacaman MJ. 2005. The bactericidal effect of silver nanoparticles. *Nanotechnology.* 1:2346–2353. doi:10.1088/0957-4484/16/10/059
- Obritsch JA, Ryu D, Lampila LE, Bullerman LB. 2008. Antibacterial effects of long-chain polyphosphates on selected spoilage and pathogenic bacteria. *J Food Prot.*71:1401–1405. doi:10.4315/0362-028X-71.7.1401
- Pal S, Tak YK, Song JM. 2007. Does the antibacterial activity of silver nanoparticles depend on the shape of the nanoparticle? A study of the Gram-negative bacterium *Escherichia coli*. *Appl Environ Microbiol.* 73:1712–1720. doi:10.1128/ AEM.02218-06
- Reidy B, Haase A, Luch A, Dawson KA, Lynch I. 2013. Mechanisms of silver nanoparticle release, transformation and toxicity: a critical review of current knowledge and recommendations for future studies and applications. *Materials (Basel).* 6:2295–2350. doi:10.3390/ma6062295
- Shibata H, Morioka T. 1982. Antibacterial action of condensed phosphates on the bacterium *Streptococcus mutans* and experimental caries in the hamster. *Arch Oral Biol.* 27:809– 816. doi:10.1016/0003-9969(82)90034-6
- Silva S, Henriques M, Oliveira R, Williams D, Azeredo J. 2010. *In vitro* biofilm activity of non-*Candida albicans* *Candida* species. *Curr Microbiol.* 61:534–540. doi:10.1007/s00284-010-9649-7
- Silva S, Pires P, Monteiro DR, Negri M, Gorup LF, Camargo ER, Barbosa DB, Oliveira R, Williams DW, Henriques M, Azeredo J. 2013. The effect of silver nanoparticles and nystatin on mixed biofilms of *Candida glabrata* and *Candida albicans* on acrylic. *Med Mycol.* 51:178–184. doi:10.3109/13693786.2012.700492
- Souza JA, Amaral JG, Moraes JC, Sasaki KT, Delbem AC. 2013. Effect of sodium trimetaphosphate on hydroxyapatite solubility: an *in vitro* study. *Braz Dent J.* 24:235–240. doi:10.1590/0103-6440201302000

Takeshita EM, Danelon M, Castro LP, Sasaki KT, Delbem AC. 2015. Effectiveness of a toothpaste with low fluoride content combined with trimetaphosphate on dental biofilm and enamel demineralization *in situ*. *Caries Res.* 49:394–400. doi:10.1159/000381960

Vaara M, Jaakkola J. 1989. Sodium hexametaphosphate sensitizes *Pseudomonas aeruginosa*, several other species of *Pseudomonas*, and *Escherichia coli* to hydrophobic drugs. *Antimicrob Agents Chemother.* 33:1741–1747. doi:10.1128/AAC.33.10.1741

Table 1 - MIC values of each composite and the controls tested against the two microorganisms

Composites and controls	MIC ($\mu\text{g Ag/ml}$)	
	<i>Streptococcus mutans</i>	<i>Candida albicans</i>
T1	-	-
T10	40	10
H1	80	80
H10	40	10
AgNP	125	62.5
CHG	0.93	3.75
F	125	-
TMP	-	-
HMP	6.25	12.5
AgNO ₃	12.5	3.15

Figure 1 - XRD patterns of commercial TMP (a) and HMP powder (b) and the synthesized nanocomposites, respectively.

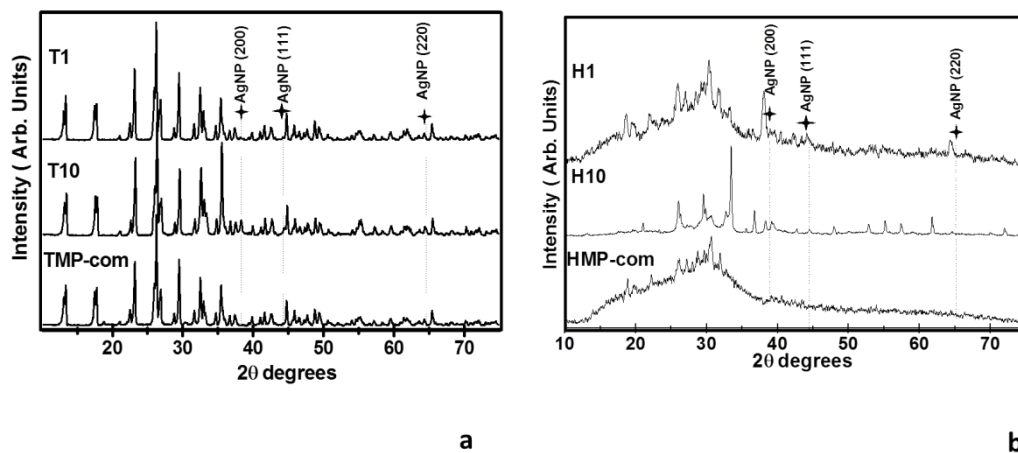


Figure 2 - SEM images and EDX mapping in 2-D at different magnifications of T10 (a and b) and H10 (c and d). Arrows indicate AgNP dispersed on TMP and HMP surfaces. Red dots show silver distribution on phosphates.

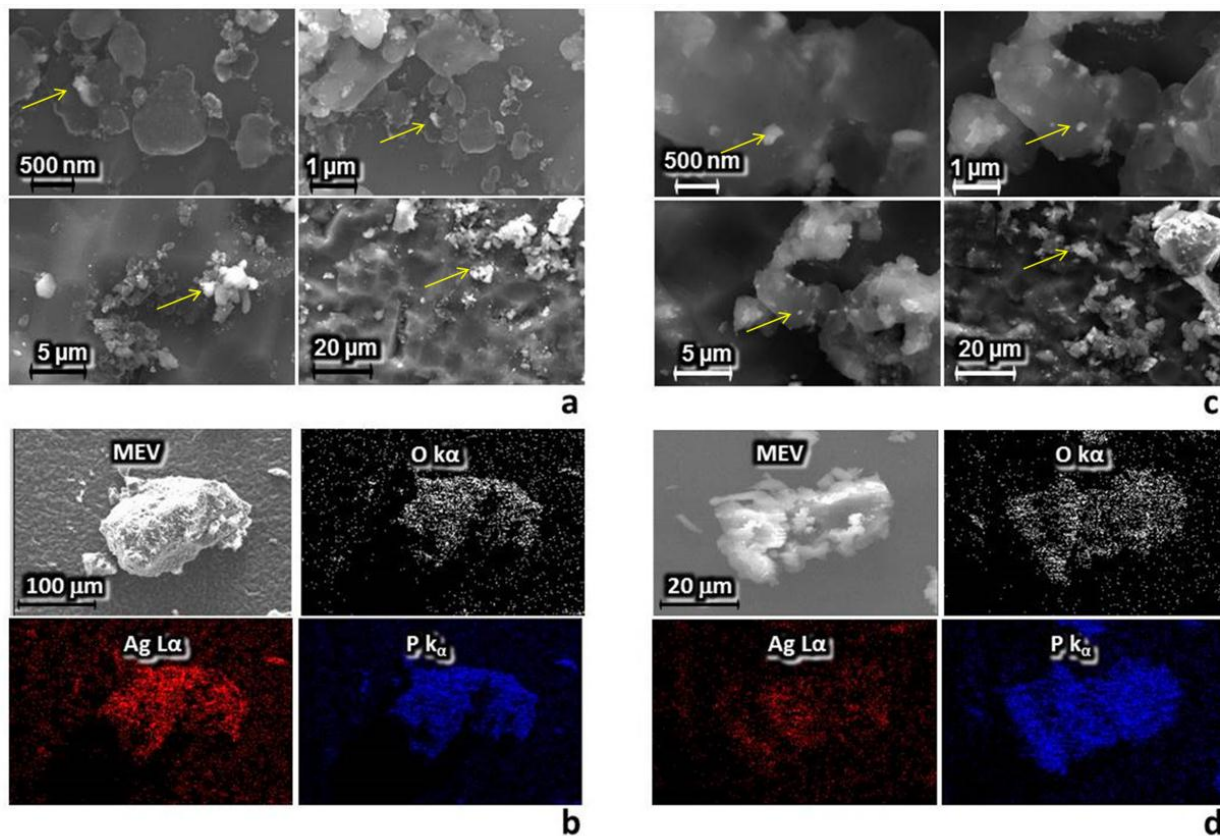


Figure 3 - a) Logarithm (mean \pm dp) of colony forming units normalized by adhesion area (\log_{10} CFU cm^{-2}); (b) absorbance values per cm^2 obtained through crystal violet assay; (c) absorbance values per cm^2 obtained through XTT assay for *C. albicans* and *S. mutans* biofilms after treatment for 24 h. Bars indicate SD of the mean. Different lowercase letters represent statistical difference between groups and concentrations tested (Fisher, $p < 0.001$). NC=negative control; PC=positive control (CHG); T10=TMP-AgNP10%; H10=HMP-AgNP10%.

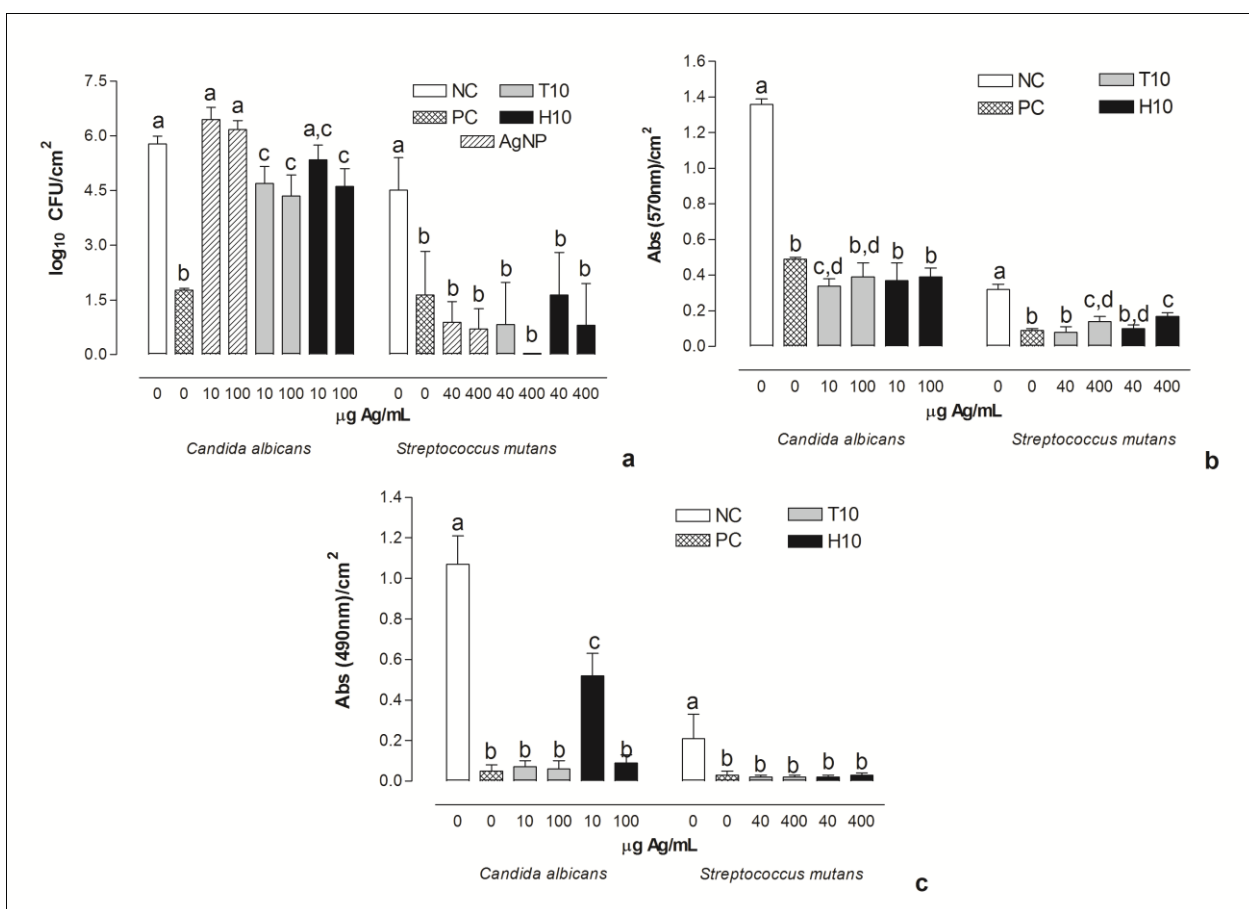


Figure 4 - SEM images of *C. albicans* biofilms: (a) negative control; (b) positive control; (c) T10 ($10 \mu\text{gAg ml}^{-1}$); (d) T10 ($100 \mu\text{gAg ml}^{-1}$); (e) H10 ($10 \mu\text{gAg ml}^{-1}$); (f) H10 ($100 \mu\text{gAg ml}^{-1}$)

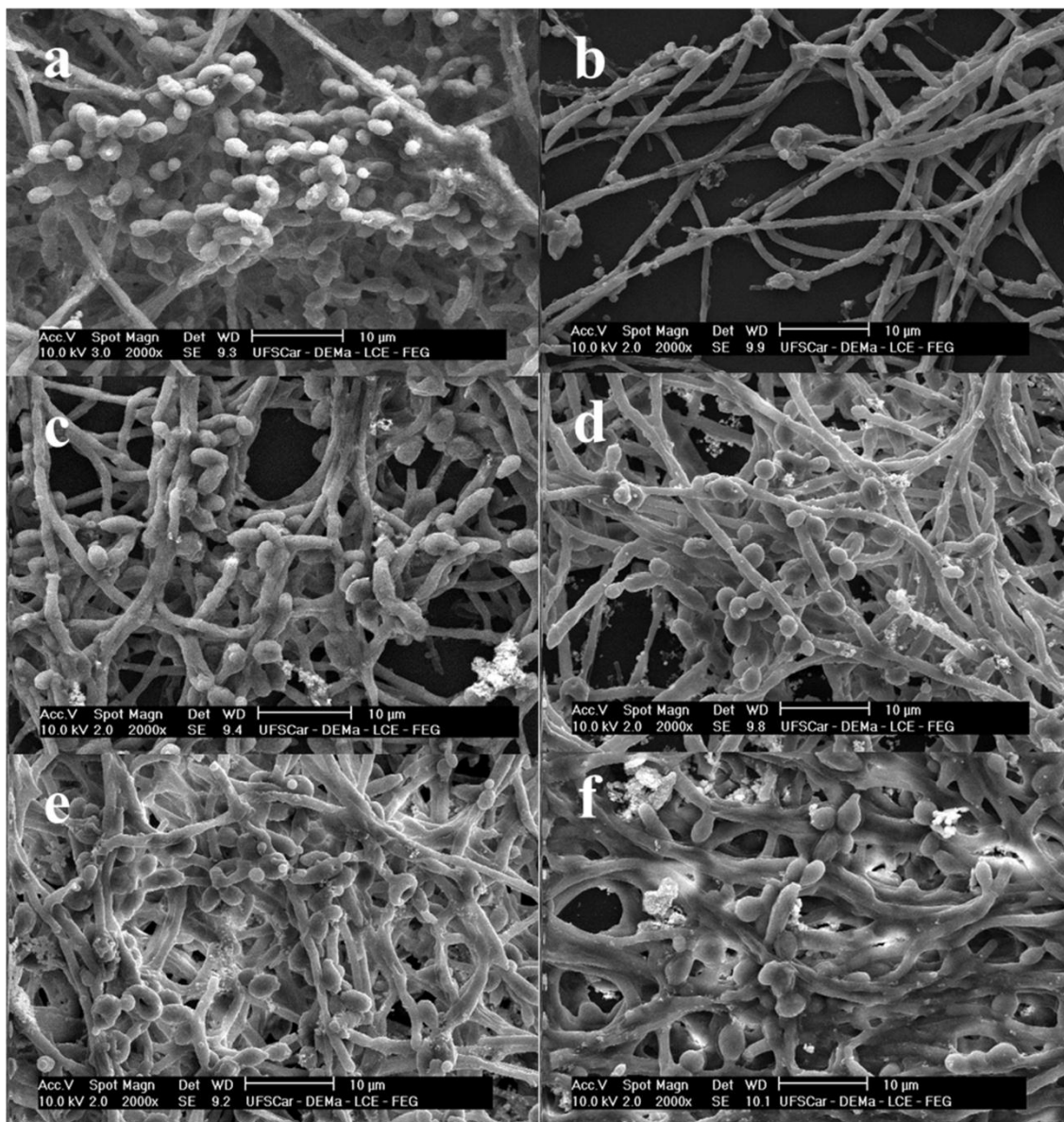
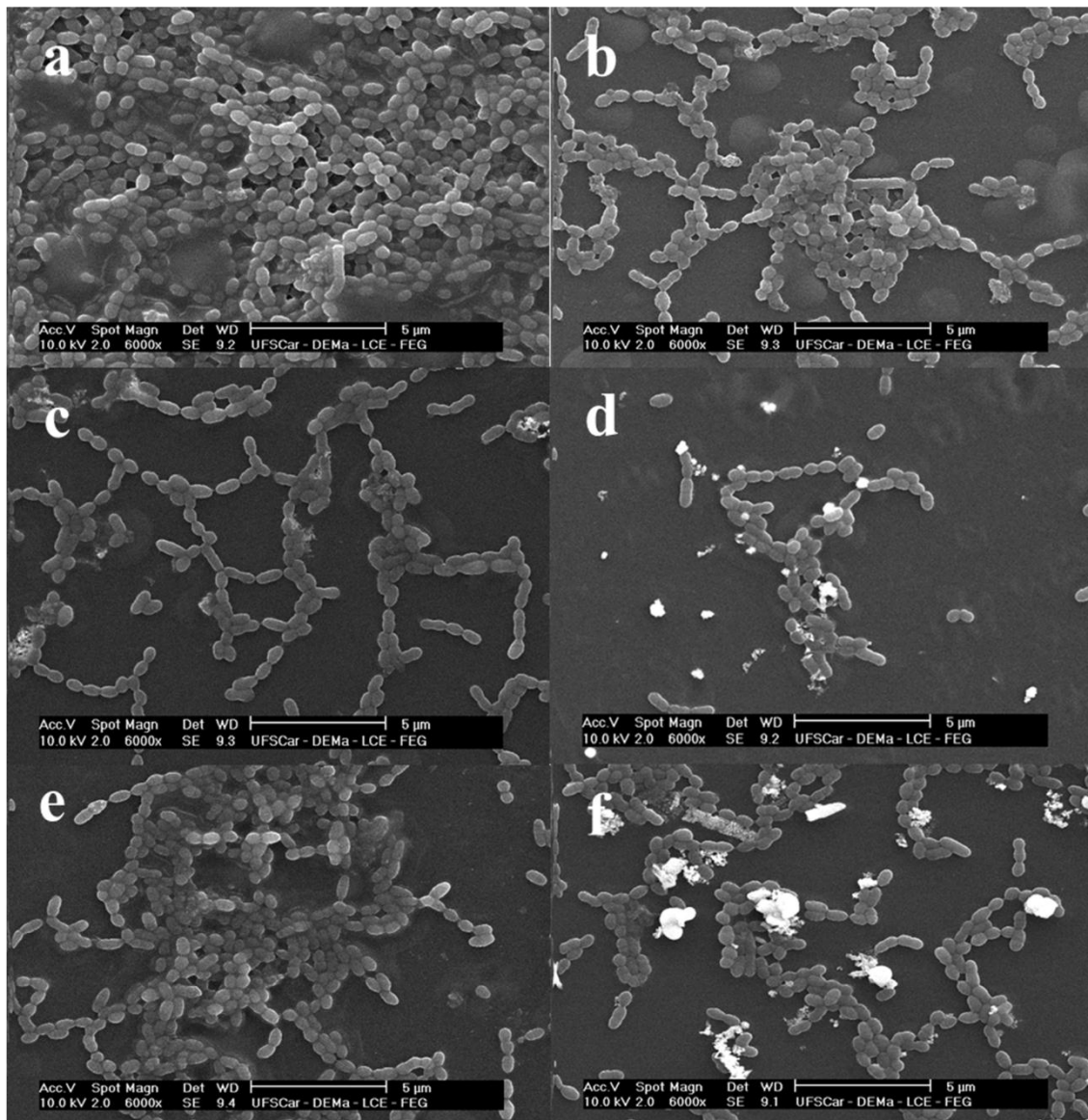


Figure 5 - SEM images of *S. mutans* biofilms: (a) negative control; (b) positive control; (c) T10 ($40 \mu\text{gAg ml}^{-1}$); (d) T10 ($400 \mu\text{gAg ml}^{-1}$); (e) H10 ($40 \mu\text{gAg ml}^{-1}$); (f) H10 ($400 \mu\text{gAg ml}^{-1}$)



Capítulo 2

***In vitro* evaluation of a composite containing sodium trimetaphosphate,
fluoride and silver nanoparticles on enamel demineralization and its
antibiofilm activity against oral pathogens**

**Artigo adequado às normas do periódico Caries Research*

***In vitro* evaluation of a composite containing sodium trimetaphosphate, fluoride and silver nanoparticles on enamel demineralization and antibiofilm activity against oral pathogens**

ABSTRACT

Objective: This study developed a nanocomposite of sodium trimetaphosphate (TMP), fluoride (F) and silver nanoparticles (Ag) and evaluated its effect on enamel demineralization using pH-cycling model, and its effectiveness in single and mixed biofilm formation of *Candida albicans* (ATCC 10231) and *Streptococcus mutans* (ATCC 25175). **Methods:** The nanocomposite contains the following compounds 0.2% TMP, 100 ppm F, and 10% Ag (100F/TMP/Ag). Bovine enamel blocks (4 mm x 4 mm, n=60) selected by the initial surface hardness (SHi) were followed allocated (n=12): deionized water (Placebo), 100ppmF (100F), 225 ppmF (225F), 100ppmF + 0.2%TMP (100F/TMP) and 100 ppmF + 0.2%TMP + 10%Ag (100F/TMP/Ag). Blocks were treated twice a day, and submitted to five pH cycles (demineralizing/remineralizing solutions). The surface hardness loss (%SH), integrated loss of subsurface hardness (Δ KHN), fluoride (F) and calcium (Ca) in enamel were measured. The anti-biofilm effect of 100F/TMP/Ag was assessed through counting of colony forming units (CFUs), and structural analyzed by scanning electron microscopy. **Results:** 225F, 100F/TMP and 100F/TMP Ag showed similar values of %SH ($p > 0.001$). 225F, 100F/TMP and 100F/TMP/Ag groups were able to reduce the lesion body (Δ KHN) in the depth of 5-20 μ m. F concentration in enamel was similar for 100F/TMP/Ag and 225F ($p > 0.001$). 100F, 225F, 100F/TMP and 100F/TMP/Ag presented the highest and the same concentration of Ca ($p > 0.001$). 100F/TMP/Ag promoted significant reduction ($p < 0.001$) of cultivable cells of *S. mutans* of 5.42 and 4.46 \log_{10} in single and mixed biofilms respectively, while *C. albicans* demonstrated more resistance. **Conclusion:** The addition of Ag to F/TMP did not interfere on the demineralization of enamel surface and inhibits significantly the biofilm formation regarding to the main relevant bacteria of dental caries, stimulating researches including its use in prevention or treatment of carious lesions.

Keywords: Dental caries; Polyphosphates; Silver nanoparticles; Biofilms

INTRODUCTION

Dental caries is a multifactorial disease and can be considered as a consequence of the metabolic activity of the microorganisms present in the dental biofilm specially the microorganisms that produce acids, as consequence of their expression of factors of virulence [Krzysciak et al., 2014]. The presence of biofilm on dental surface is the indispensable factor for the development of this disease [Nyvad et al., 2013]. It is known that *Streptococcus mutans* is the main microorganism involved in the occurrence of caries, since it is capable of producing acids and survive in this environmental, synthesizing polysaccharides and decreasing the oral pH, being these important virulence factors that lead to the demineralization of dental enamel [Fejerskov O, 2005]. *Candida albicans*, a fungus species frequently found in the oral cavity, plays an significant role as a secondary agent and it is strong involved in the progression of the caries process, since this fungus has the capacity to produce enzymes as factors of virulence, specially the proteolytic enzymes which contribute to collagenolysis, particularly in dentinal caries [Pereira et al., 2018].

In this sense, silver, present an antimicrobial effect in broad-spectrum [Xiu et al., 2012], and has been tested as antimicrobial agent [Balazs et al., 2004; Bjarnsholt et al., 2007; Monteiro et al., 2009; Panacek et al., 2006] in wound dressings, burn treatments, creams, and coatings on medical devices to prevent the microorganism colonization on the surfaces of these materials. In its nanoparticulate form, silver particles (AgNP) have showed considerable antimicrobial efficacy for allowing greater contact of its volume and so increasing its interaction with bacteria and fungi [Lok CN, 2006; Morones et al., 2005].

The anticaries activity of phosphate salts, specially sodium trimetaphosphate (TMP), has already been considered effective against enamel demineralization [Danelon et al., 2014; Manarelli et al., 2011; Takeshita et al., 2016; Takeshita et al., 2015; Takeshita et al., 2011]. Takeshita et al (2011).[Takeshita et al., 2011] confirmed the potential of TMP as a preventive agent of caries, particularly in cases where fluoride use should be limited. Danelon et al (2014).[Danelon et al., 2014], it is ensured that the sodium trimetaphosphate supplied with different concentrations of fluoride (F) was able to decrease the mineral loss and increase the remineralization process, due to

its ability to modify the surface of the hydroxyapatite through its adsorption. The inhibition of in vitro enamel demineralization was also demonstrated using TMP associated to F in mouth rinse by Favretto et al (2013) .[Favretto et al., 2013].

Thinking in controlling dental caries by inhibiting the demineralization process and modulating oral pathogenic biofilms , it would be opportune to develop a composite containing TMP, F and AgNP. So, the objective of this study was to synthesize and characterize a nanocomposite with TMP, F, and AgNP, and to verify its effect on tooth enamel demineralization as well as its antimicrobial action in single and dual species of biofilms of *Candida albicans* and *Streptococcus mutans*.

MATERIALS AND METHODS

Synthesis and characterization of sodium trimetaphosphate, fluoride and silver nanoparticles

The synthesis of the nanocomposite with sodium trimetaphosphate (TMP), fluoride (F) and silver nanoparticles (AgNP) was performed on an alcoholic medium (isopropanol) using sodium borohydride (NaBH_4 , Sigma-Aldrich, St. Louis, MO, USA) as a reductor agent, following the protocol proposed by Miranda et al (2010). [Miranda M, 2010] with some modifications. Suspensions containing sodium trimetaphosphate (TMP, Sigma-Aldrich, CAS 7785-84 4), fluoride (NaF , Merck, Darmstadt, Germany) and silver nitrate (AgNO_3 , Merck) were prepared in the presence of surfactant (ammonium salt of polymethacrylic acid (NHPM), Polysciences, Inc., Warrington, PA, USA). AgNO_3 was employed at 10% of the weight of TMP. The molar proportions between TMP and F was 1.23 : 1 respectively. The nanocomposite was stove-dried overnight at 70°C in . The size and morphology of 100F/TMP/Ag (Figure 1) and TMP (Figure 2) were investigated by transmission electron microscopy using HRTEM TECNAI F 20 Microscope operating at 200 kV. The samples were dispersed in isopropanol and deposited onto a carbon coated grid. The 2-D images were constructed by analyzing the P K α and Ag L α 1 energy emissions through Energy Dispersive Spectroscopy (EDS).

Compounds formulation and fluoride assessment

The nanocomposite previously synthesized containing 0.2% TMP, Ag at 10% and 100 ppm F (100F/TMP/Ag) were diluted in deionized water. The control solutions used were deionized water, 100 and 225 ppm F (as NaF, Merck, CAS 7681-49-4, Germany). A solution containing 0.2% TMP, 100 ppm F (100F/TMP) was also prepared. F concentrations [Delbem et al., 2009] of the groups containing or not Ag were checked prior to the beginning of the study.

Experimental Design for pH-cycling

Enamel blocks (4 mm × 4 mm, n=60) were obtained from bovine incisors kept in formaldehyde 2% pH 7.0 for 30 days prior to experimental procedures [Delbem and Cury, 2002]. Blocks were selected by initial surface hardness test (SHi; 320 to 380 KHN) and randomly divided in five experimental solutions (n=12 each). They were submitted to a pH-cycling regimen (5 days) and to treatments (twice a day) with the following solutions: deionized water (Placebo), 100 ppm F (100F), 225 ppm F (225F), 100 ppm F plus TMP at concentration of 0.2% (100F/TMP) and 100 ppm F plus TMP at concentration of 0.2% plus Ag at 10% (100F/TMP/Ag). Next, final surface hardness (SHf), integrated loss subsurface hardness (Δ KHN), enamel fluoride (F), calcium (Ca) concentration were determined.

pH-cycling and treatment with solutions

The blocks were submitted to five pH cycles during five days (one cycle/day), and immersed in a fresh remineralizing solution for two additional days [Vieira et al., 2005]. They were immersed under constant stirring in each specific solution (1 mL) when removed from the demineralizing (6 hours – Ca and P 2,0 mmol L⁻¹ in acetate buffer 0,075 mol L⁻¹, 0,04 µg F/mL in pH 4,7 – 2,2 mL/mm²) and from the remineralizing solutions (18 hours – Ca 1.5 mmol L⁻¹, P 0.9 mmol L⁻¹, KCl 0.15 mol L⁻¹ in cacodylic buffer 0.02 mol L⁻¹, 0.05 µg F/mL in pH 7,0 – 1,1 mL/mm²). The blocks were washed with deionized water for 30 seconds.

Analysis of enamel hardness

Surface hardness was determined with Micromet 5114 hardness tester (Buehler, Lake Bluff, USA) and Buehler Omni Met software (Buehler, Lake Bluff,

USA) with a Knoop diamond indenter under a 25 g load for 10s. Five indentations, separated by a distance of 100 μm , were made in the center of each block to analyze initial surface hardness (SHi). After the pH-cycling, final surface hardness (SHf) was calculated by producing five other indentations (100 μm from the baseline indentations). For cross-sectional hardness measurements, blocks were sectioned at the center and one of the halves was included in acrylic resin and gradually polished until the enamel was totally exposed. One sequence of 14 indentations were created at different distances (5, 10, 15, 20, 25, 30, 40, 50, 70, 90, 110, 130, 220, and 330 μm) from the surface of the enamel, in the central region of the blocks, using a Micromet 5114 hardness tester (Buehler Lake Bluff, IL, USA) with a Knoop diamond indenter under a 5-g load for 10 s. Integrated hardness (KHN $\times \mu\text{m}$) for the lesion into sound enamel was calculated by the trapezoidal rule (GraphPad Prism, version 3.02) and subtracted from the integrated hardness for sound enamel to obtain the integrated area of the subsurface regions in enamel, which was named integrated loss of subsurface hardness (ΔKHN ; KHN $\times \mu\text{m}$) [Spiguel et al., 2009].

Analysis of F and Ca concentration in the enamel

Blocks (n=12/per group, 2 mm \times 2 mm) were obtained from the halves of the original 4 mm \times 4 mm specimens not embedded, and fixed with adhesive glue on a mandrel for straight. Self-adhesive polishing discs (diameter, 13 mm) and 400-grit silicon carbide (Buehler) were fixed to the bottom of polystyrene crystal tube (J-10; Injeplast, São Paulo, SP, Brazil). One layer of $50.0 \pm 0.03 \mu\text{m}$ each enamel block was removed. The vials, after the addition of 0.5 ml HCl 1.0 mol L⁻¹, were kept under constant stirring for 1 hour [Weatherell et al., 1985], modified by Alves et al. [Alves et al., 2007]. For F analysis, specific electrode 9409BN (Thermo Scientific, Beverly, MA, USA) and microelectrode reference (Analyser, São Paulo, Brazil) coupled to an ion analyzer (Orion 720A+, Thermo Scientific, Beverly, MA, USA) was used. The electrodes were calibrated with standards containing from 0.25 to 4.00 $\mu\text{g F/mL}$ (100 ppm F, Orion 940907), under the same conditions as the samples. The readings were conducted using 0.25 mL of the biopsy solution, buffered with the same volume of TISAB II modified NaOH [Akabane et al., 2018]. The results were expressed in $\mu\text{g/mm}^3$.

Calcium (Ca) analysis was performed using the Arsenazo III colorimetric method [Vogel et al., 1983]. The absorbance readings were recorded at 650 nm by using a plate reader (PowerWave 340, Biotek, Winooski, VT, USA). The results were expressed as mg/mm³.

Biofilm formation and treatment

Biofilms from single and mixed cultures were cultured in 96-well microtiter plates (Costar®, Corning Incorporated, Tewksbury, MA, USA). Each well received 200 µl of *C. albicans* (ATCC 10231) cell suspension (1×10^7 ml⁻¹ cells in artificial saliva), according to the methodology by Silva et al. [Silva et al., 2010], and 200 µl of *S. mutans* (ATCC 25175) cell suspension (1×10^8 ml⁻¹ cells in artificial saliva), following the study of Arias et al. [Arias et al., 2016], for the formation of simple biofilms. For biofilms of mixed species, 100 µl of each suspension (2×10^7 ml⁻¹ cells of *C. albicans* plus 2×10^8 cells ml⁻¹ of *S. mutans*) was dispensed into each well. The plates were incubated at 37 ° C for 2 h for biofilm adhesion. After this time, the wells containing biofilm were washed once with 200 µl of phosphate buffered saline (PBS; pH 7, 0.1 M) to remove non-adherent cells. Subsequently, the treatment was carried out by adding 200 µl of artificial saliva containing 100F/TMP/Ag at 40 µg ml⁻¹. For positive and negative control were used 0.018% Chlorhexidine Gluconate (CHG; Periogard, Colgate Palmolive Industrial Ltda, Sao Paulo, Brazil) and artificial saliva. The biofilms were then incubated at 37°C for 24 h.

Biofilm quantification

The colony-forming unit counting test (CFUs) was used to quantify the single and mixed biofilms of *C. albicans* and *S. mutans*. For thus, biofilm-containing wells were scraped and the suspensions were vortexed and serially diluted in PBS and plated on SDA (*C. albicans*), BHI (*S. mutans*). For mixed biofilm, microorganisms were plated on CHROMagar (Difco) (*C. albicans*) and BHI supplemented with amphotericin B (Sigma-Aldrich) (*S. mutans*) [Fernandes et al., 2016]. After this, the agar plates were incubated at 37° C during 24 h for *C. albicans* and 48h for *S. mutans*. In the next step the number of CFUs was counted and log CFU per unit area (log₁₀ CFU cm⁻²) was determined. The tests were performed independently and in triplicate.

Microscopy

The SEM (scanning electron microscopy) was performed to visualize changes in the structure of the simple and mixed biofilms submitted to the treatment with the nanocomposite. Single and mixed biofilms were formed in 24-well plates as described above. Briefly, after cell adhesion period, the nanocomposite, positive and negative controls were added to the wells as previously described. After 24 h, the wells were gently washed once with PBS and the biofilms were dehydrated according to the protocol of Silva et al (2013).[Silva et al., 2013]. The bottom of each well containing the biofilms was then cut with a flame-sterilized scalpel blade (number 11, Solidor, Lamedid Comercial e Serviços Ltda, Barueri, Brazil). After this, the samples received a gold bath and SEM analysis was performed (S-360 microscope, Leo, Cambridge, MA, USA) [Fernandes et al., 2016].

Statistical analysis

The analyzes of pH-cycling were performed using SigmaPlot software (version 12.0) (Systat Software Inc., San Jose, CA, USA) and the level of statistical significance was set at 5%. The variables% SH and F did not present normal distribution (Shapiro-Wilk) and homogeneous (Cochran test) and were submitted to Kruskal-Wallis followed by the Student-Newman-Keuls comparison test. The Ca values were homogeneous (log₁₀ transformation) and were submitted to analysis of variance at a criterion followed by the Student-Newman-Keuls test. For the variable Δ KHN, treatments and areas were considered as variables of variation. The results showed normal and homogeneous distribution and were submitted to analysis of variance at two criteria followed by the Student-Newman-Keuls test. For the biofilm analysis, SigmaPlot 12.0 software was also used with a significance level of 5%. The quantification of the colony forming units (CFUs) of the simple and mixed biofilms passed the Shapiro-Wilks test of normal and homogeneous distribution and were subjected to One Way Analysis of Variance. After all the paired data were submitted to a multiple comparison protocol by the Holm-Sidak method.

RESULTS

Synthesis and characterization the nanocomposite

TEM show images of association between silver nanoparticles with sodium trimetaphosphate (TMP). Figure 1 shows silver nanoparticles anchoring on the surface of the TMP, in a dispersed and uncrosslinked form.

The Histogram of TEM image (Figure 1-B) demonstrate the mean size of the Ag nanoparticles was 11 nm. Figure 1-A shows silver nanoparticles (gray shades) dispersed and decorating the surface of the phosphates at micrometric size (white shades)(Figure 1-C). The 2D images were constructed by analyzing the energy released from the P K α (constituents of the TMP material) (Figure 1-D) and Ag K α (Figure 1-E) emissions, indicating the uniform distribution of these elements in the demarcated area in the micrograph.

The Histogram and Energy Dispersive Spectroscopy (EDS) of the commercial TMP indicated the mean size of 72nm and the presence of sodium (Na), oxygen (O), phosphorus (P) (Figure 2).

Analysis of superficial (%SH) and transversal hardness (Δ KHN), F and Ca concentrations

The mean pH of all solutions was 7.9 (SD 0.1). The mean SH of blocks was 360.0 (SD 9.8) KHN ($p = 0,533$). No significant differences were observed among the groups after random allocation ($p = 0.474$).

The use of 225F solution resulted in a 40% decrease in %SH in comparison with 100F (Table 1). The demineralization of the enamel surface was the similar in samples treated with solution containing 225F, 100F/TMP and 100/TMP/Ag (table 1) ($p > 0.001$). In addition, the capacity to reduce the lesion body (Δ KHN) was higher with 110F, 225F, 100F/TMP and 100F/TMP/Ag ($p < 0.001$) in zone A (5–20 μ m) and similar in zone B for 225F and 100F/TMP. The 100F/TMP/Ag group had greater demineralization in zone B (20–130 μ m) ($p < 0.001$) (Figure 3).

A dose-response pattern was observed between F concentrations in the solutions not supplemented with TMP/Ag and enamel fluoride uptake. The addition of TMP/Ag to the solution did not influence enamel F concentration, so that its effect was similar to 225F, except for the Placebo, 100F and 100F/TMP which showed a lower concentration ($p < 0.001$). The 100F, 225F, 100F/TMP

and 100F/TMP/Ag groups had the highest and similar Ca concentration ($p > 0.001$), followed by Placebo.

Antimicrobial effect

Figure 4 shows 100F/TMP/Ag nanocomposite afforded expressive reductions of *S. mutans* cultivables cells of 5.42 and 4.46 \log_{10} respectively in single and mixed biofilms. Indeed, those reductions were statistically similar to the reduction promoted by chlorhexidine gluconate (PC) regardless if *S. mutans* grew in the presence or not of *C. albicans*. Figure 4 also suggests *S. mutans* was more tolerant to both 100F/TMP/Ag and PC when its biofilm was formed in the presence of *C. albicans*, increasing the *S. mutans* cell viability from 0.70 to 2.29 \log_{10} and from 1.23 to 2.52 \log_{10} . It is also noted that *C. albicans* was more resistant to 100F/TMP/Ag and PC in mixed biofilms, increasing the viable cells in 0.63 and 1.14 \log_{10} respectively. Although 100F/TMP/Ag has reduced less than 0.5 \log_{10} the viable cells of *C. albicans* in both single and mixed biofilms, the 100F/TMP/Ag effectiveness was considered statically significant when compared to the negative control.

Microscopy

Figure 5 shows the treatment with 100F/TMP/Ag nanocomposite was effective against single and mixed biofilms of *C. albicans* and *S. mutans*, and similar to the reduction obtained with treatment with chlorhexidine gluconate (positive control).

DISCUSSION

The present study showed that the nanocomposite synthesized demonstrated an anticarie and antimicrobial potential.

The ability of inhibition of demineralization was determined by an in vitro model that simulates the caries dynamics through pH cycling [Vieira et al., 2005]. The concentration of TMP and F chosen was based on previous studies [Favretto et al., 2013; Manarelli et al., 2011] where mouth rinse containing 100ppmF associated with 0.2% TMP also obtained similar results to the mouth rinse containing 225 ppm of F against artificial caries lesions [Favretto et al.,

2013]. Even featuring no significant difference concentrations of fluoride in the enamel as well as in the present study compared to 100 ppm F group, the surface and cross-sectional hardness were similar to 225 ppm F group. The association of TMP to 100 ppm F has shown that TMP does not further the uptake fluoride in the hydroxyapatite [Souza et al., 2013]. Nevertheless it was observed an exponential reduction of the loss of Ca when immersed in acid solution [Amaral et al., 2018; Souza et al., 2013]. The effect of TMP can be related to its capacity to hinder acid diffusion into the enamel [Akabane et al., 2018; Moretto et al., 2013; Takeshita et al., 2011] due to two possible reasons. First, the formulation with 100 ppm F only reduced the mineral loss in relation to placebo with no significance difference of F, and lower Ca, present in the enamel when compared to 100F/0.2% TMP group (Table 1). Second, TMP does not enhance the deposition of calcium fluoride [Souza et al., 2013], but associated to 100 ppm F increased the protective effect against enamel erosion [Manarelli et al., 2011]. TMP is adsorbed making a layer on enamel [Akabane et al., 2018; Amaral et al., 2018] that alters the selective permeability and diffusion of ions into the inner enamel [Akabane et al., 2018; Takeshita et al., 2011]. This can explain the lower mineral loss in the deeper of the enamel (Zone B: Table 1 and Figure 1) and concentration of Ca (Table 1) in the enamel like the 225 ppm F.

The addition of the silver nanoparticles (AgNP) to the nanocomposite was aimed to add antimicrobial action to TMP-F proportion proven effective against enamel demineralization. The concentration of AgNP was based on Mendes-Gouvêa et al (2018) [Mendes-Gouvea et al., 2018] In the present study, it was found that the addition of silver nanoparticles did not affect the demineralization inhibition property of the enamel surface when associated to TMP/F, since %SH and Δ KHN at zone A (5 – 20 μ m; Table 1 and Figure 1) presented similar values compared to a conventional 225 ppm F solution. The same occurred in relation to the amount of F and Ca at ~50 μ m of depth from the surface of the enamel (table 1) for 100F/TMP/Ag solution, which obtained values were close to the solution of 225 ppm F. The best effect of the group 225 ppm F compared to 100 ppm F was dependent of the F uptake in the enamel. In the case of 100F/0.2% TMP, it was dependent on the ability of TMP to reduce the acid diffusion into the enamel. However, it appears that the product

deposited from the nanocomposite on the outer layer of the enamel does not avoid deep mineral loss in the enamel. Probably, the product formed with Ag may have a restricted effect on the outermost layer of the enamel and, when associated with TMP, may affect its adsorption on the enamel.

Although there are no studies showing the association of Ag, TMP and F, other studies have already tested the action of the Ag with F in the enamel demineralization and remineralization [Delbem et al., 2006; Liu et al., 2012; Nozari et al., 2017; Punyanirun et al., 2018; Zhi et al., 2013]. These studies agree that mechanism of action of Ag/F is due to deposition of calcium fluoride and silver phosphate on enamel. This coating formed on enamel from of the Ag and F would work as a source of F and PO₄ inducing the precipitation of fluorapatite and producing superior enamel remineralization [Punyanirun et al., 2018; Zhi et al., 2013]. Nevertheless, the majority of studies do not show an additional effect of Ag when associated with F [Delbem et al., 2006; Liu et al., 2012; Zhi et al., 2013], mainly in the deeper region of the enamel. The studies that show an adjunct effect of Ag analyzed the enamel by micro-computed tomography [Punyanirun et al., 2018] or only determined the surface hardness [Nozari et al., 2017]. Indeed, the Ag ions which penetrated into the enamel [Liu et al., 2012; Nozari et al., 2017; Zhi et al., 2013] may be responsible by the increase in mineral density in depth of the lesions not signifying true remineralization [Liu et al., 2012; Zhi et al., 2013]. It seems that the deposits of Ag and F formed would produce a great mineralization in the outer of the enamel as observer in the present study (zone A: 5 – 20 µm; Table 1 and Figure1).

Nevertheless, these layers do not hinder acid diffusion into the enamel and the mineral loss in the inner of the enamel (zone B: 20 – 130 µm). It is important to say that the studies cited above used Ag in its ionic form at 38% and the present study tested nanocomposites with silver nanoparticles at 10%. Thus, the products formed on enamel from the nanocomposite may contain differences that influenced the results. Of the three groups with similarity in the %SH results (Table 1) showed no difference in the concentration of calcium in the enamel. However, the higher presence of fluoride in the enamel was observed for formulation with more F (225 ppm F) or with AgNP added (100/TMP/Ag). Despite this, the greater mineral loss with the nanocomposite in

depth in the enamel can be explained by two probable reasons. First, the presence of AgNP in the TMP/F formulation may have reduced the TMP adsorption on the enamel. TMP is able to hinder acid penetration into the enamel as described above. Second, the layer formed by products from AgNP and F did not block acid diffusion since the mineral loss in the deeper of the lesion occurred. However, nanocomposite should be tested in *in situ* and *in vivo* studies since it presented the antimicrobial effect and the mineral loss may be lower than observed in the pH-cycling model.

It is worth mentioning that one of the limitations of *in vitro* pH cycling models is that it can not represent with fidelity the complex reactions that occur in the oral environment. In this study, we sought to correlate the effect of enamel demineralization reduction with the ability to inhibit the formation of biofilms by microorganisms responsible for acid secretion that results in caries lesion. Thus, we tested this compound against simple and mixed biofilms of the bacterial specie *Streptococcus mutans* and the fungal specie *Candida albicans*.

The association of sodium trimetaphosphate (TMP), fluoride (F) and AgNPs was able to produce a nanocomposite with antimicrobial action against the formation of biofilms of two important oral pathogens *Candida albicans* and *Streptococcus mutans*, regardless if it were in single or dual species forms. The results of our previous study [Mendes-Gouvea et al., 2018] demonstrated the association of TMP-Ag did not reduce the inhibition potential of AgNP against *C. albicans* and *S. mutans*. Conversely, the highest effectiveness was displayed when AgNP were in TMP in particular against *S. mutans*. It is noteworthy that 100F/TMP/Ag was also expressively effective to prevent the biofilm growth of *S. mutans*, reducing more than 99.999% the biofilm formation of this Gram positive bacteria. This highest inhibitory biofilm growth could be ascribed to alteration of the surface of AgNP when associated with TMP, producing more imperfections on there and the increase of the AgNP reactivity which leads on disruption of some molecules, and hence enabling the 'membranolytic effect' when in contact with microorganisms cells [Richter et al., 2017]. It is also known that AgNP may adhere to the microorganism outer membrane [Li et al., 2008] or the Ag⁺ released could break the membrane [M., 2013], leading to intracellular damages and death of the cell. The concentration of Ag in 100F/TMP/Ag was the same used in our previous work [Mendes-Gouvea et al., 2018] of 40 µg/mL and could

be able to reduce 4.2 log₁₀ 24h old- biofilm cells of *S. mutans*. The difference between the results in inhibiting the biofilm growth of *S. mutans* and *C. albicans* may either credited by the increase of the permeability of the external membrane of *S. mutans* by 100F/TMP/Ag due to the sequestration of divalent cations by TMP [Akhtar et al., 2008; Maier et al., 1999; Mendes-Gouvea et al., 2018; Obritsch et al., 2008] that would permit the passage of Ag into the membranes and so damage to the bacterial cell by DNA replication loss and inactivation of some proteins [Feng et al., 2000; Mendes-Gouvea et al., 2018]. Further one, the higher efficacy of 100F/TMP combined with AgNP against *S. mutans* might be due to the buffer effect promoted by that polyphosphate, increasing the pH of the acidic environment of *S. mutans* biofilm and so interfering on its development [Mendes-Gouvea et al., 2018].

Although AgNP with no F/TMP had not been compared with 100F/TMP/Ag, our previous study could demonstrate TMP increased the action of AgNP against single 24h old-biofilms of both microorganisms *C. albicans* (ATCC 10231) and *S. mutans* (ATCC 25175). Again, *S. mutans* cells were more susceptible to TMP-AgNP nanocomposite than cells of *C. albicans*, and it could be explained by the change of the AgNP crystallographic surface structures when it is in combination with TMP [Mendes-Gouvea et al., 2018; Pal et al., 2007]. The TEM images elucidate how AgNP are arranged in the compound. They are anchored in a dispersive way on the TMP surface, and it could confirm the modification on the crystallography physical-chemical property of AgNP.

In spite of the preliminary anti-biofilm formation experiment performed in this study, of note should be the antibacterial potential demonstrated by 100F/TMP/Ag especially considering the low concentration of Ag and the relevance role of *S. mutans* in the dental caries process. Likewise, since both pathogens *S. mutans* and *C. albicans* present virulence factors on progressive caries, it is of relevance to control their presence in the oral cavity. The nanocomposite produced in the present study aggregate the properties of TMP and F in reducing the demineralization process on enamel surface as well as the antimicrobial action of Ag. Further studies with in situ and in vivo approaches are strongly encouraged in the sense of confirming the therapeutic potential of TMP and other polyphosphates/F associated with AgNP in

preventing the most prevalent chronic oral disease in whole world, which is the dental caries.

REFERENCES

- Akabane S, Delbem AC, Pessan J, Garcia L, Emerenciano N, Goncalves DF, Danelon M: In situ effect of the combination of fluoridated toothpaste and fluoridated gel containing sodium trimetaphosphate on enamel demineralization. *Journal of dentistry* 2018;68:59-65.
- Akhtar S, Paredes-Sabja D, Sarker MR: Inhibitory effects of polyphosphates on clostridium perfringens growth, sporulation and spore outgrowth. *Food microbiology* 2008;25:802-808.
- Alves KM, Pessan JP, Brighenti FL, Franco KS, Oliveira FA, Buzalaf MA, Sasaki KT, Delbem AC: In vitro evaluation of the effectiveness of acidic fluoride dentifrices. *Caries research* 2007;41:263-267.
- Amaral JG, Pessan JP, Souza JAS, Moraes JCS, Delbem ACB: Cyclotriphosphate associated to fluoride increases hydroxyapatite resistance to acid attack. *Journal of biomedical materials research Part B, Applied biomaterials* 2018.
- Arias LS, Delbem AC, Fernandes RA, Barbosa DB, Monteiro DR: Activity of tyrosol against single and mixed-species oral biofilms. *Journal of applied microbiology* 2016;120:1240-1249.
- Balazs DJ, Triandafillu K, Wood P, Chevolut Y, van Delden C, Harms H, Hollenstein C, Mathieu HJ: Inhibition of bacterial adhesion on pvc endotracheal tubes by rf-oxygen glow discharge, sodium hydroxide and silver nitrate treatments. *Biomaterials* 2004;25:2139-2151.
- Banas JA: Virulence properties of streptococcus mutans. *Frontiers in bioscience : a journal and virtual library* 2004;9:1267-1277.
- Bjarnsholt T, Kirketerp-Moller K, Kristiansen S, Phipps R, Nielsen AK, Jensen PO, Hoiby N, Givskov M: Silver against pseudomonas aeruginosa biofilms. *APMIS : acta pathologica, microbiologica, et immunologica Scandinavica* 2007;115:921-928.
- da Camara DM, Miyasaki ML, Danelon M, Sasaki KT, Delbem AC: Effect of low-fluoride toothpastes combined with hexametaphosphate on in vitro enamel demineralization. *Journal of dentistry* 2014;42:256-262.
- Danelon M, Takeshita EM, Peixoto LC, Sasaki KT, Delbem ACB: Effect of fluoride gels supplemented with sodium trimetaphosphate in reducing demineralization. *Clinical oral investigations* 2014;18:1119-1127.
- Delbem AC, Bergamaschi M, Sasaki KT, Cunha RF: Effect of fluoridated varnish and silver diamine fluoride solution on enamel demineralization: Ph-cycling study. *Journal of applied oral science : revista FOB* 2006;14:88-92.
- Delbem AC, Cury JA: Effect of application time of apf and naf gels on microhardness and fluoride uptake of in vitro enamel caries. *American journal of dentistry* 2002;15:169-172.
- Delbem AC, Sasaki KT, Vieira AE, Rodrigues E, Bergamaschi M, Stock SR, Cannon ML, Xiao X, De Carlo F, Delbem AC: Comparison of methods for evaluating mineral loss: Hardness versus synchrotron microcomputed tomography. *Caries research* 2009;43:359-365.
- do Amaral JG, Sasaki KT, Martinhon CC, Delbem AC: Effect of low-fluoride dentifrices supplemented with calcium glycerophosphate on enamel demineralization in situ. *American journal of dentistry* 2013;26:75-80.

- Favretto CO, Danelon M, Castilho FC, Vieira AE, Delbem AC: In vitro evaluation of the effect of mouth rinse with trimetaphosphate on enamel demineralization. *Caries research* 2013;47:532-538.
- Fejerskov O KE: Cárie dentária: A doença e seu tratamento clínico. . Editora São Paulo 2005.
- Feng QL, Wu J, Chen GQ, Cui FZ, Kim TN, Kim JO: A mechanistic study of the antibacterial effect of silver ions on escherichia coli and staphylococcus aureus. *Journal of biomedical materials research* 2000;52:662-668.
- Fernandes RA, Monteiro DR, Arias LS, Fernandes GL, Delbem AC, Barbosa DB: Biofilm formation by candida albicans and streptococcus mutans in the presence of farnesol: A quantitative evaluation. *Biofouling* 2016;32:329-338.
- Gauger A, Mempel M, Schekatz A, Schafer T, Ring J, Abeck D: Silver-coated textiles reduce staphylococcus aureus colonization in patients with atopic eczema. *Dermatology* 2003;207:15-21.
- Hamada S, Slade HD: Biology, immunology, and cariogenicity of streptococcus mutans. *Microbiological reviews* 1980;44:331-384.
- Huang L, Xu QA, Liu C, Fan MW, Li YH: Anti-caries DNA vaccine-induced secretory immunoglobulin a antibodies inhibit formation of streptococcus mutans biofilms in vitro. *Acta pharmacologica Sinica* 2013;34:239-246.
- Keyes PH: The infectious and transmissible nature of experimental dental caries. Findings and implications. *Archives of oral biology* 1960;1:304-320.
- Khundkar R, Malic C, Burge T: Use of acticoat dressings in burns: What is the evidence? *Burns : journal of the International Society for Burn Injuries* 2010;36:751-758.
- Klein MI, Hwang G, Santos PH, Campanella OH, Koo H: Streptococcus mutans-derived extracellular matrix in cariogenic oral biofilms. *Frontiers in cellular and infection microbiology* 2015;5:10.
- Krzysciak W, Jurczak A, Koscielniak D, Bystrowska B, Skalniak A: The virulence of streptococcus mutans and the ability to form biofilms. *European journal of clinical microbiology & infectious diseases : official publication of the European Society of Clinical Microbiology* 2014;33:499-515.
- Li Q, Mahendra S, Lyon DY, Brunet L, Liga MV, Li D, Alvarez PJ: Antimicrobial nanomaterials for water disinfection and microbial control: Potential applications and implications. *Water research* 2008;42:4591-4602.
- Liu BY, Lo EC, Li CM: Effect of silver and fluoride ions on enamel demineralization: A quantitative study using micro-computed tomography. *Australian dental journal* 2012;57:65-70.
- Lok CN HC, Chen R, He QY, Yu WY, Sun H, Tam PK, Chiu JF, Che CM: Proteomic analysis of the mode of antibacterial action of silver nanoparticles. *Journal of proteome research* 2006;5:9.
- M. KKaR: Metallic nanoparticles: Mechanism of antibacterial action and influencing factors. *J Comp Clin Pathol Res* 2013;1:160-174.
- Maier SK, Scherer S, Loessner MJ: Long-chain polyphosphate causes cell lysis and inhibits bacillus cereus septum formation, which is dependent on divalent cations. *Applied and environmental microbiology* 1999;65:3942-3949.
- Manarelli MM, Moretto MJ, Sasaki KT, Martinhon CC, Pessan JP, Delbem AC: Effect of fluoride varnish supplemented with sodium trimetaphosphate on enamel erosion and abrasion. *American journal of dentistry* 2013;26:307-312.
- Manarelli MM, Vieira AE, Matheus AA, Sasaki KT, Delbem AC: Effect of mouth rinses with fluoride and trimetaphosphate on enamel erosion: An in vitro study. *Caries research* 2011;45:506-509.
- McGaughey C, Stowell EC: Effects of polyphosphates on the solubility and mineralization of ha: Relevance to a rationale for anticaries activity. *Journal of dental research* 1977;56:579-587.

- Mendes-Gouvea CC, do Amaral JG, Fernandes RA, Fernandes GL, Gorup LF, Camargo ER, Delbem CAB, Barbosa DB: Sodium trimetaphosphate and hexametaphosphate impregnated with silver nanoparticles: Characteristics and antimicrobial efficacy. *Biofouling* 2018;1-10.
- Miranda M FA, Diaz M, Esteban-Tejeda L, Lopez-Esteban S, Malpartida F, Torrecillas R, Moya JS: Silver-hydroxyapatite nanocomposites as bactericidal and fungicidal materials. *International Journal of Material Research* 2010;101:6.
- Monteiro DR, Gorup LF, Takamiya AS, Ruvollo-Filho AC, de Camargo ER, Barbosa DB: The growing importance of materials that prevent microbial adhesion: Antimicrobial effect of medical devices containing silver. *International journal of antimicrobial agents* 2009;34:103-110.
- Moretto MJ, Delbem AC, Manarelli MM, Pessan JP, Martinhon CC: Effect of fluoride varnish supplemented with sodium trimetaphosphate on enamel erosion and abrasion: An in situ/ex vivo study. *Journal of dentistry* 2013;41:1302-1306.
- Morones JR, Elechiguerra JL, Camacho A, Holt K, Kouri JB, Ramirez JT, Yacaman MJ: The bactericidal effect of silver nanoparticles. *Nanotechnology* 2005;16:2346-2353.
- Newbrune E: *Cariology*. . Baltimore: Williams & Wilkins 1978:326.
- Nikawa H, Yamashiro H, Makihira S, Nishimura M, Egusa H, Furukawa M, Setijanto D, Hamada T: In vitro cariogenic potential of candida albicans. *Mycoses* 2003;46:471-478.
- Nozari A, Ajami S, Rafiei A, Niazi E: Impact of nano hydroxyapatite, nano silver fluoride and sodium fluoride varnish on primary teeth enamel remineralization: An in vitro study. *Journal of clinical and diagnostic research : JCDR* 2017;11:ZC97-ZC100.
- Nyvad B, Crielaard W, Mira A, Takahashi N, Beighton D: Dental caries from a molecular microbiological perspective. *Caries research* 2013;47:89-102.
- Obritsch JA, Ryu D, Lampila LE, Bullerman LB: Antibacterial effects of long-chain polyphosphates on selected spoilage and pathogenic bacteria. *Journal of food protection* 2008;71:1401-1405.
- Pal S, Tak YK, Song JM: Does the antibacterial activity of silver nanoparticles depend on the shape of the nanoparticle? A study of the gram-negative bacterium escherichia coli. *Applied and environmental microbiology* 2007;73:1712-1720.
- Panacek A, Kvitek L, Pucek R, Kolar M, Vecerova R, Pizurova N, Sharma VK, Nevecna T, Zboril R: Silver colloid nanoparticles: Synthesis, characterization, and their antibacterial activity. *The journal of physical chemistry B* 2006;110:16248-16253.
- Pereira D, Seneviratne CJ, Koga-Ito CY, Samaranayake LP: Is the oral fungal pathogen candida albicans a cariogen? *Oral diseases* 2018;24:518-526.
- Petersen PE: Challenges to improvement of oral health in the 21st century--the approach of the who global oral health programme. *International dental journal* 2004;54:329-343.
- Punyanirun K, Yospiboonwong T, Kunapinun T, Thanyasrisung P, Trairatvorakul C: Silver diamine fluoride remineralized artificial incipient caries in permanent teeth after bacterial ph-cycling in-vitro. *Journal of dentistry* 2018;69:55-59.
- Richter K, Facal P, Thomas N, Vandecandelaere I, Ramezanpour M, Cooksley C, Prestidge CA, Coenye T, Wormald PJ, Vreugde S: Taking the silver bullet colloidal silver particles for the topical treatment of biofilm-related infections. *ACS applied materials & interfaces* 2017;9:21631-21638.
- Sheiham A, James WP: Diet and dental caries: The pivotal role of free sugars reemphasized. *Journal of dental research* 2015;94:1341-1347.
- Shimotoyodome A, Kobayashi H, Tokimitsu I, Hase T, Inoue T, Matsukubo T, Takaesu Y: Saliva-promoted adhesion of streptococcus mutans mt8148 associates with dental plaque and caries experience. *Caries research* 2007;41:212-218.
- Silva S, Henriques M, Oliveira R, Williams D, Azeredo J: In vitro biofilm activity of non-candida albicans candida species. *Current microbiology* 2010;61:534-540.

- Silva S, Pires P, Monteiro DR, Negri M, Gorup LF, Camargo ER, Barbosa DB, Oliveira R, Williams DW, Henriques M, Azeredo J: The effect of silver nanoparticles and nystatin on mixed biofilms of candida glabrata and candida albicans on acrylic. *Medical mycology* 2013;51:178-184.
- Souza JA, Amaral JG, Moraes JC, Sasaki KT, Delbem AC: Effect of sodium trimetaphosphate on hydroxyapatite solubility: An in vitro study. *Brazilian dental journal* 2013;24:235-240.
- Spiguel MH, Tovo MF, Kramer PF, Franco KS, Alves KM, Delbem AC: Evaluation of laser fluorescence in the monitoring of the initial stage of the de-/remineralization process: An in vitro and in situ study. *Caries research* 2009;43:302-307.
- Takeshita EM, Castro LP, Sasaki KT, Delbem AC: In vitro evaluation of dentifrice with low fluoride content supplemented with trimetaphosphate. *Caries research* 2009;43:50-56.
- Takeshita EM, Danelon M, Castro LP, Cunha RF, Delbem AC: Remineralizing potential of a low fluoride toothpaste with sodium trimetaphosphate: An in situ study. *Caries research* 2016;50:571-578.
- Takeshita EM, Danelon M, Castro LP, Sasaki KT, Delbem AC: Effectiveness of a toothpaste with low fluoride content combined with trimetaphosphate on dental biofilm and enamel demineralization in situ. *Caries research* 2015;49:394-400.
- Takeshita EM, Exterkate RA, Delbem AC, ten Cate JM: Evaluation of different fluoride concentrations supplemented with trimetaphosphate on enamel de- and remineralization in vitro. *Caries research* 2011;45:494-497.
- Tamura S, Yonezawa H, Motegi M, Nakao R, Yoneda S, Watanabe H, Yamazaki T, Senpuku H: Inhibiting effects of streptococcus salivarius on competence-stimulating peptide-dependent biofilm formation by streptococcus mutans. *Oral microbiology and immunology* 2009;24:152-161.
- Ten Cate JM: In vitro studies on the effects of fluoride on de- and remineralization. *Journal of dental research* 1990;69 Spec No:614-619; discussion 634-616.
- Ulkur E, Oncul O, Karagoz H, Yeniz E, Celikoz B: Comparison of silver-coated dressing (acticoat), chlorhexidine acetate 0.5% (bactigrass), and fusidic acid 2% (fucidin) for topical antibacterial effect in methicillin-resistant staphylococci-contaminated, full-skin thickness rat burn wounds. *Burns : journal of the International Society for Burn Injuries* 2005;31:874-877.
- Vaara M, Jaakkola J: Sodium hexametaphosphate sensitizes pseudomonas aeruginosa, several other species of pseudomonas, and escherichia coli to hydrophobic drugs. *Antimicrobial agents and chemotherapy* 1989;33:1741-1747.
- Van Dijk JW BJ, Driessens FC: The effect of some phosphates and a phosphonate on the electrochemical properties of bovine enamel. *Archives of oral biology* 1980; 25.
- Vieira AE, Delbem AC, Sasaki KT, Rodrigues E, Cury JA, Cunha RF: Fluoride dose response in pH-cycling models using bovine enamel. *Caries research* 2005;39:514-520.
- Vogel GL, Chow LC, Brown WE: A microanalytical procedure for the determination of calcium, phosphate and fluoride in enamel biopsy samples. *Caries research* 1983;17:23-31.
- Weatherell JA, Robinson C, Strong M, Nakagaki H: Micro-sampling by abrasion. *Caries research* 1985;19:97-102.
- Xiu ZM, Zhang QB, Puppala HL, Colvin VL, Alvarez PJ: Negligible particle-specific antibacterial activity of silver nanoparticles. *Nano letters* 2012;12:4271-4275.
- Zhi QH, Lo EC, Kwok AC: An in vitro study of silver and fluoride ions on remineralization of demineralized enamel and dentine. *Australian dental journal* 2013;58:50-56.

Table 1. Mean values (SD) of percentage loss of surface hardness (% SH), integrated loss of subsurface hardness (Δ KHN) and chemical elements present in enamel according to treatments (n = 12)

Treatments	Analysis				
	*%SH (KHN)	** Δ KHN (KHN \times μ m)		Elements in the enamel (μ g/mm ³)	
		&Zone A (5 – 20 μ m)	&Zone B (20 – 130 μ m)	*F	**Ca
Placebo	-85.0 ^a (5.9)	4,269.1 ^{a,A} (232.9)	4,173.4 ^{a,A} (1,020.5)	0.88 ^a (0.36)	187.5 ^a (31.7)
100F	-61.1 ^b (12.5)	2,998.7 ^{b,A} (611.9)	4,207.0 ^{a,B} (1,025.9)	1.32 ^b (0.54)	212.1 ^a (41.0)
225F	-41.9 ^c (4.6)	2,551.5 ^{b,A} (724.8)	2,373.2 ^{b,A} (926.7)	1.71 ^c (0.65)	258.4 ^b (24.7)
100F/TMP	-42.3 ^c (3.5)	2,181.5 ^{b,A} (525.2)	2,185.2 ^{b,A} (1,157.8)	1.19 ^b (0.52)	311.1 ^b (95.1)
100F/TMP/Ag	-43.0 ^c (8.1)	2,427.6 ^{b,A} (480.6)	4,279.2 ^{a,B} (1,035.4)	1.59 ^c (0.49)	310.9 ^b (74.1)

Different lowercase letters indicate significant difference between groups in each analysis. Different upper case letters indicate difference between zones A and B for Δ KHN values in each treatment. View the profile in longitudinal section in Figure 1. (*) Kruskal-Wallis (p <0.001), Student-Newman-Keuls. (**) ANOVA (p <0.001), Student-Newman-Keuls.

Figure 1 - (A) TEM image of sodium trimetaphosphate decorated with silver nanoparticles (TMP-Ag); (B) Histogram of TEM image of Ag nanoparticles; (C) TEM images in a specific area of TMP-Ag nanoparticles; (D) EDS mapping in 2D presented a quantity of Potassium; (E) EDS mapping in 2D presented a dense quantity of silver distributed in the TMP-Ag nanoparticles

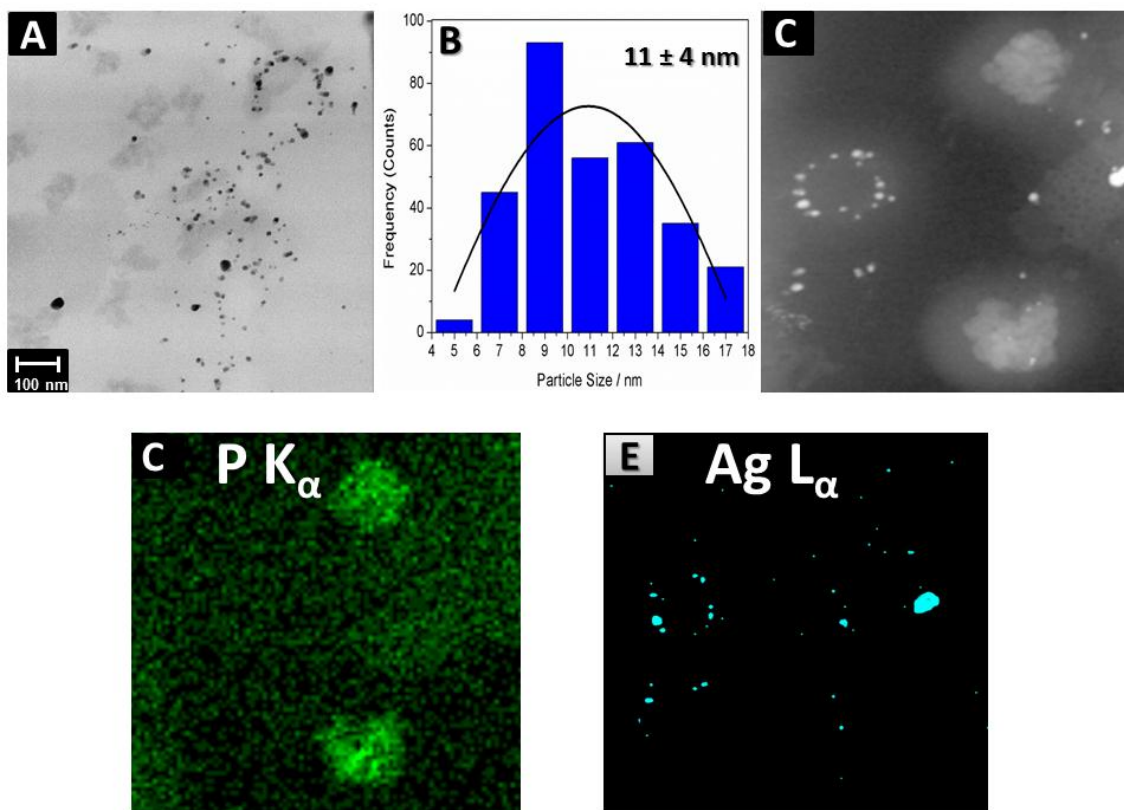


Figure 2 – (A) TEM image of sodium trimetaphosphate (TMP) nanoparticles; (B) Histogram of TEM image of TMP nanoparticles and (C) Energy Dispersive Spectroscopy (EDS) of TMP nanoparticles

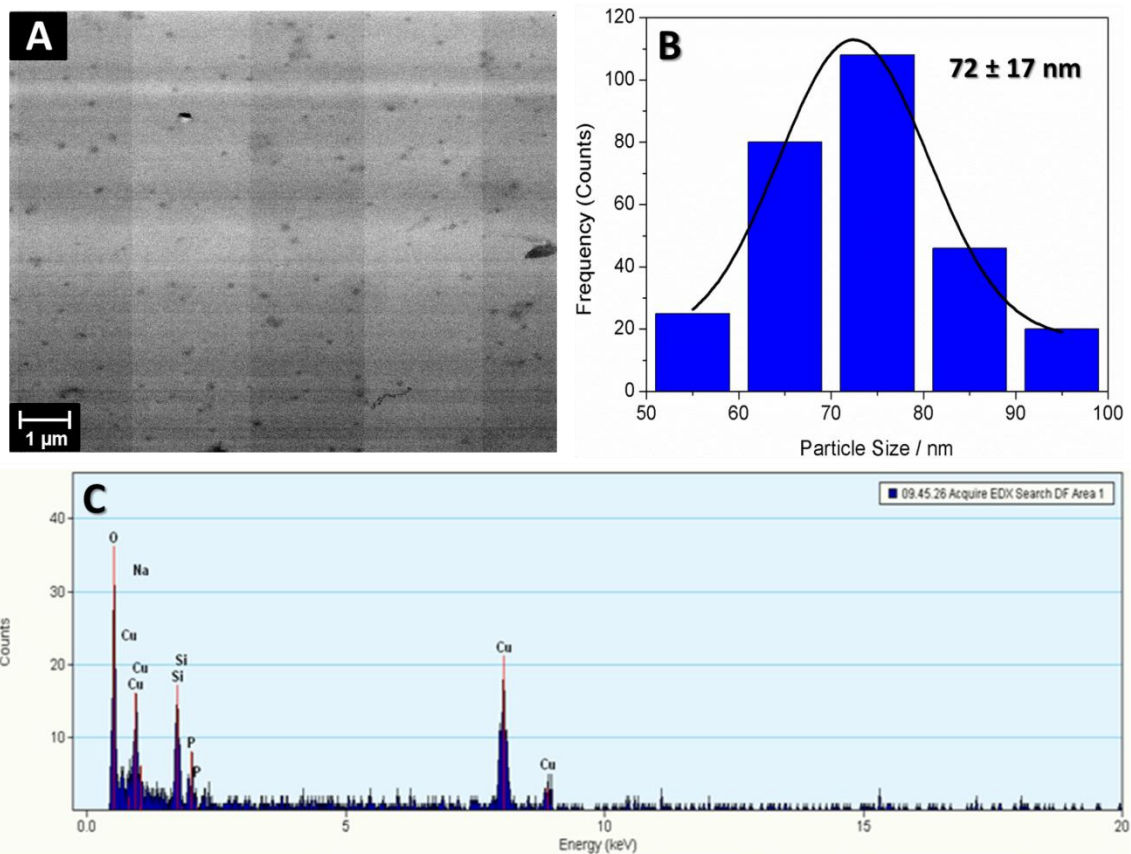


Figure 3 - Profile of the hardness in longitudinal section (mean KHN, n = 12) as a function of the enamel depth according to the treatments. Values and comparisons between zones A and B are described in Table 1.

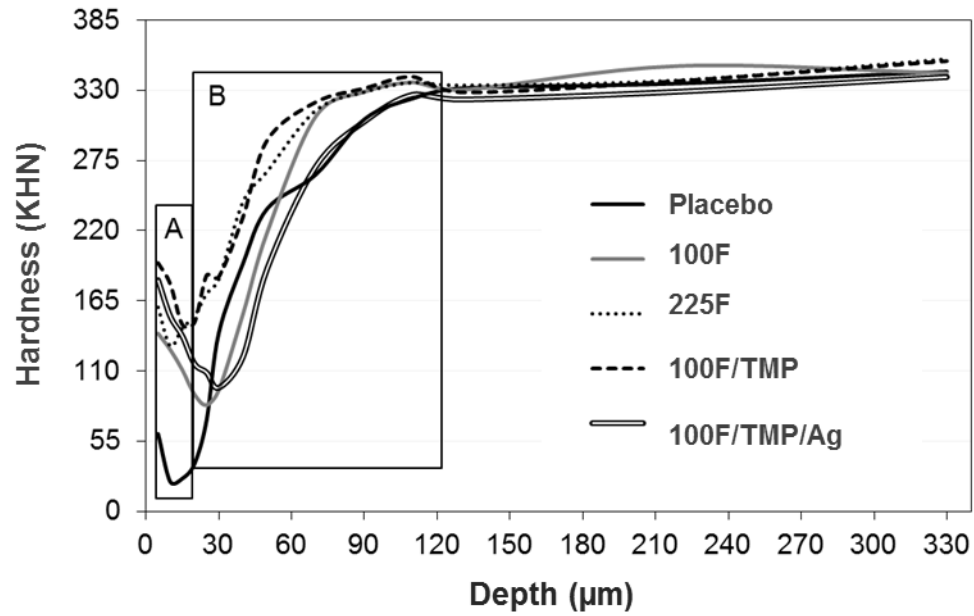


Figure 4 - Logarithm (mean \pm SD) of colony forming units normalized by adhesion area (\log_{10} CFU cm^{-2}) for *C. albicans* and *S. mutans* biofilms (single and mixed) after treatment for 24 h. Bars indicate SD of the mean. Different letters represent statistical difference among the groups (Holm-Sidak method, $p < 0.001$). NC=negative control; PC=positive control (CHG); TMP=100F/TMP/Ag

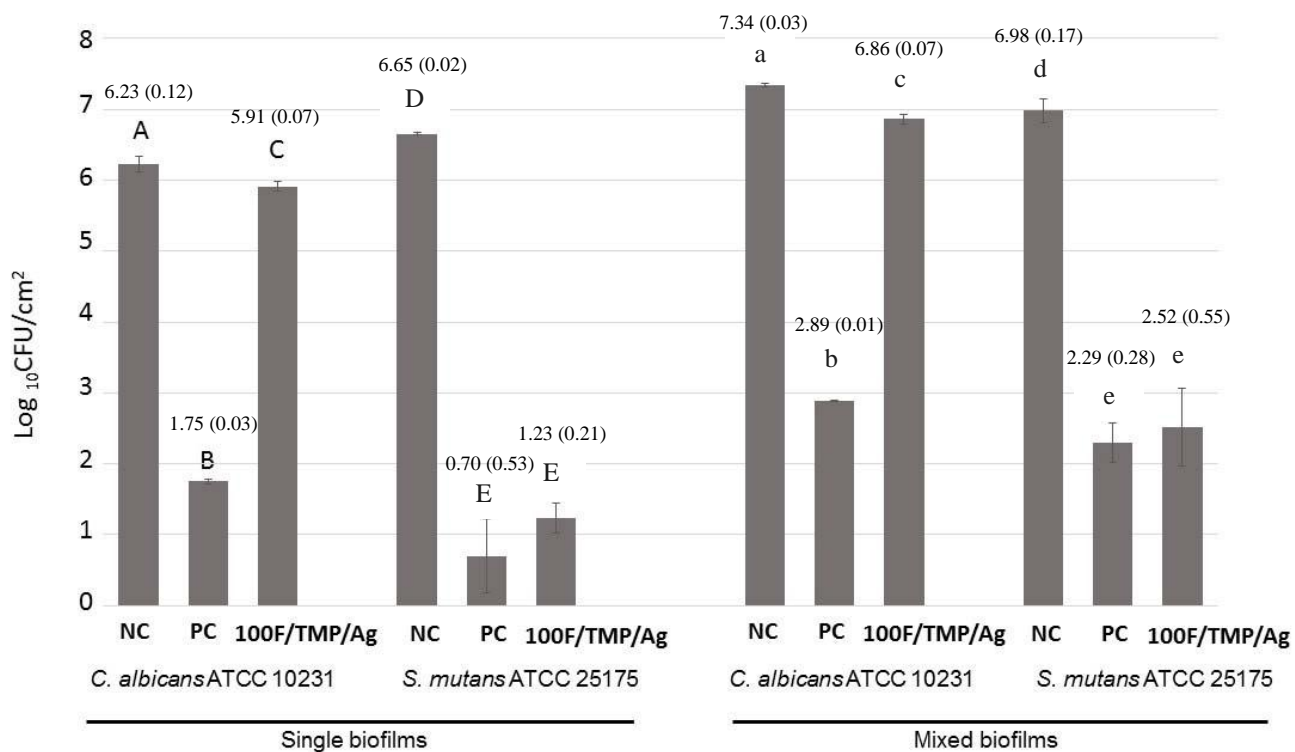
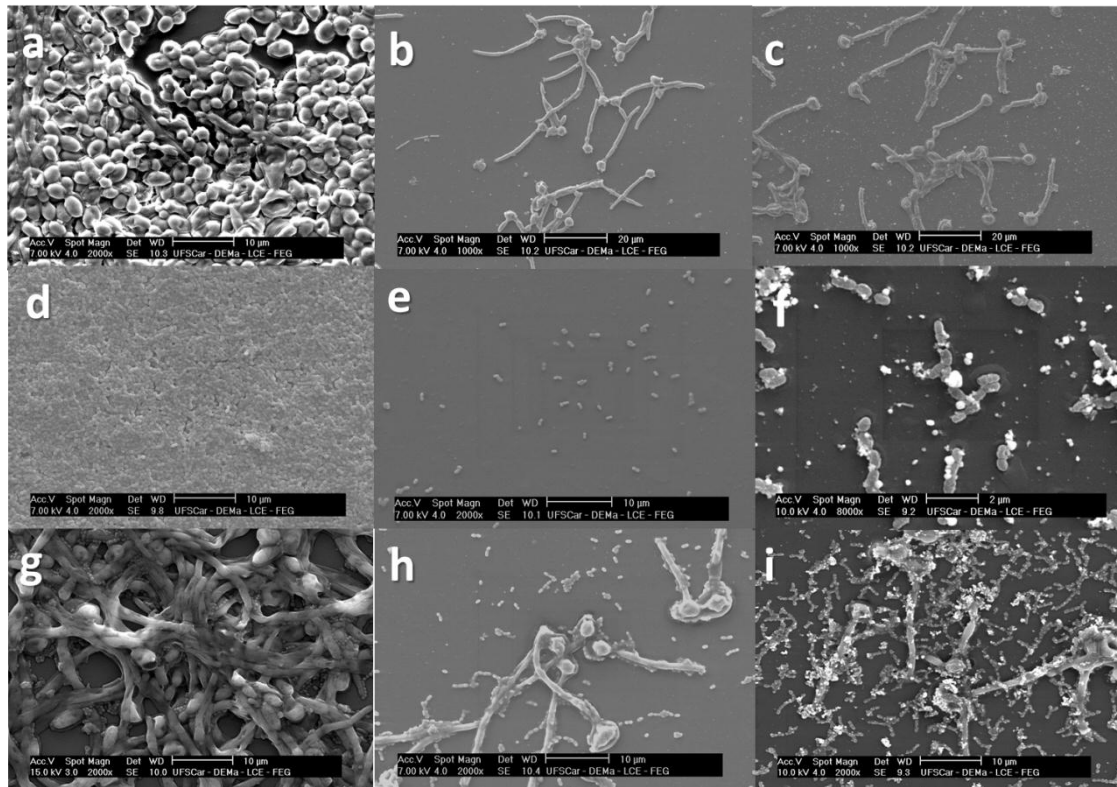



Figure 5 - SEM images of: *C. albicans* biofilms - (a) negative control, (b) positive control, (c) TMP 0,2%/F/Ag 10%; *S. mutans* biofilms - (d) negative control, (e) positive control, (f) TMP 0,2%/F/Ag 10%; mixed biofilms (*C. albicans* + *S. mutans*) - (g) negative control; (h) positive control; (i) TMP 0,2%/F/Ag 10%.



ANEXO

Sodium trimetaphosphate and hexametaphosphate Impregnated with silver nanoparticles: characteristics and antimicrobial efficacy

Carla Corrêa Mendes-Gouvêa^a, Jackeline Gallo do Amaral^b, Renan Aparecido Fernandes^b,
 Gabriela Lopes Fernandes^b, Luiz Fernando Gonup^c, Emerson Rodrigues Camargo^c,
 Carlos Alberto Botazzo Delbem^c  and Debora Barros Barbosa^b

^aDepartment of Pediatric Dentistry and Public Health, School of Dentistry Araçatuba, São Paulo State University (UNESP), Araçatuba, Brazil;

^bDepartment of Dental Materials and Prosthodontics, School of Dentistry Araçatuba, São Paulo State University (UNESP), Araçatuba, Brazil;

^cDepartment of Chemistry, Federal University of São Carlos (UFSCar), São Carlos, Brazil

ABSTRACT

This study aimed to synthesize and characterize materials containing silver nanoparticles (AgNP) with polyphosphates (sodium trimetaphosphate (TMP) or sodium hexametaphosphate (HMP), and evaluate their effect against *Candida albicans* and *Streptococcus mutans*. The minimum inhibitory concentration (MIC) was determined, which was followed by the quantification of the biofilm by counting colony-forming units (CFUs), the amount of metabolic activity, and the total biomass. The MICs revealed greater effectiveness of composites containing 10% Ag (TMP + Ag10% (T10) and HMP + Ag10% (H10)) against both microorganisms. It was observed that T10 and H10 reduced the formation of biofilms by 56–76% for *C. albicans* and by 52–94% for *S. mutans* for total biomass and metabolic activity. These composites promoted significant log reductions in the number of CFUs, between 0.45–1.43 log₁₀ for *C. albicans* and 2.88–3.71 log₁₀ for *S. mutans* ($p < .001$). These composites demonstrated significant antimicrobial activity, especially against *S. mutans*, and may be considered a potential alternative for new dental materials.

ARTICLE HISTORY

Received 15 August 2017
 Accepted 31 January 2018

KEYWORDS

Polyphosphates; silver nanoparticles; biofilms; *Candida albicans*; *Streptococcus mutans*

Introduction

Streptococcus mutans is the main cariogenic microorganism, and its capacity to produce acid and survive at low pH, as well as its ability to synthesize extracellular polysaccharides, are important virulence factors which contribute to the colonization of the tooth surface, development of pathogenic biofilms, and enamel demineralization (Leone et al. 2008, Li and Chang 2008, Delbem et al. 2014). Although the development of dental caries is related to the formation of biofilm, the progression of established lesions may include species of *Candida*, particularly *Candida albicans* (Shibata and Morioka 1982; Monteto et al. 2015).

Composites containing calcium and phosphate have shown promising anticariostatic effects (do Amaral et al. 2013; Takeshita et al. 2015; da Camara et al. 2016). Among the phosphate salts, sodium trimetaphosphate (TMP) and sodium hexametaphosphate (HMP) have been effective in reducing enamel demineralization and improving remineralization. They are inorganic cyclophosphates with the capacity to adsorb hydroxyapatite and protein through

hydroxyl (Souza et al. 2013; Delbem et al. 2014) and amino (Leone et al. 2008; Li and Chang 2008) attachment sites. Added to low concentrations of fluoride in an appropriate proportion in oral health products, they provide a greater protective effect than conventional fluoride products (da Camara et al. 2014; Manarelli et al. 2015; Takeshita et al. 2015; Concetcao et al. 2015; da Camara et al. 2016).

The development of multifunctional biomaterials to be used in the health field is the focus of increasing attention. Added to that, the exponential growth of nanotechnology, and the use of silver nanoparticles (AgNP) as an antimicrobial agent allowing for increased surface-to-volume ratios and specific interactions with species of bacteria and fungi (Baker et al. 2005; Morones et al. 2005; Lok et al. 2006), new approaches could be useful to prevent and control dental caries. A material containing AgNP as an antimicrobial agent, and sources of fluoride and phosphate to prevent the demineralization of dental enamel, could achieve promising results. Thus, this study aimed to synthesize composites containing AgNP, F, and TMP or HMP, and to characterize and evaluate their effect against *Streptococcus mutans* and *Candida albicans*.

Candida albicans BIOFILME SIMPLES**One Way Analysis of Variance**

Data source: Data 1 in c13 ca cfu

Dependent Variable: Col 2

Normality Test (Shapiro-Wilk) Passed (P = 0,577)

Equal Variance Test: Passed (P = 0,381)

Group Name	N	Missing	Mean	Std Dev	SEM
CN	3	0	6,227	0,142	0,0823
CP	3	0	1,750	0,0293	0,0169
TMP	3	0	5,915	0,0888	0,0513

Source of Variation	DF	SS	MS	F	P
Between Groups	2	37,491	18,746	1936,529	<0,001
Residual	6	0,0581	0,00968		
Total	8	37,549			

The differences in the mean values among the treatment groups are greater than would be expected by chance; there is a statistically significant difference (P = <0,001).

Power of performed test with alpha = 0,050: 1,000

All Pairwise Multiple Comparison Procedures (Holm-Sidak method):

Overall significance level = 0,05

Comparisons for factor: Col 1

Comparison	Diff of Means	t	P	P<0,050
CN vs. CP	4,477	55,737	<0,001	Yes
TMP vs. CP	4,165	51,845	<0,001	Yes
CN vs. TMP	0,313	3,892	0,008	Yes

Streptococcus mutans BIOFILME SIMPLES**One Way Analysis of Variance**

Data source: Data 1 in c13 ca cfu

Dependent Variable: Col 2

Normality Test (Shapiro-Wilk) Passed (P = 0,555)

Equal Variance Test: Passed (P = 0,089)

Group Name	N	Missing	Mean	Std Dev	SEM
CN	3	0	6,654	0,0212	0,0122
CP	3	0	0,702	0,644	0,372
TMP	3	0	1,232	0,258	0,149

Source of Variation	DF	SS	MS	F	P
Between Groups	2	65,101	32,550	202,420	<0,001
Residual	6	0,965	0,161		
Total	8	66,065			

The differences in the mean values among the treatment groups are greater than would be expected by chance; there is a statistically significant difference (P = <0,001).

Power of performed test with alpha = 0,050: 1,000

All Pairwise Multiple Comparison Procedures (Holm-Sidak method):

Overall significance level = 0,05

Comparisons for factor: **Col 1**

Comparison	Diff of Means	t	P	P<0,050
CN vs. CP	5,952	18,178	<0,001	Yes
CN vs. TMP	5,422	16,559	<0,001	Yes
TMP vs. CP	0,530	1,618	0,157	No

Candida albicans BIOFILME MISTO**One Way Analysis of Variance**

Data source: Data 1 in c13 ca cfu

Dependent Variable: Col 2

Normality Test (Shapiro-Wilk) Passed (P = 0,427)

Equal Variance Test: Passed (P = 0,443)

Group Name	N	Missing	Mean	Std Dev	SEM
CN	3	0	7,343	0,0366	0,0211
CP	3	0	2,885	0,00656	0,00378
TMP	3	0	6,861	0,0849	0,0490

Source of Variation	DF	SS	MS	F	P
Between Groups	2	35,915	17,957	6275,023	<0,001
Residual	6	0,0172	0,00286		
Total	8	35,932			

The differences in the mean values among the treatment groups are greater than would be expected by chance; there is a statistically significant difference (P = <0,001).

Power of performed test with alpha = 0,050: 1,000

All Pairwise Multiple Comparison Procedures (Holm-Sidak method):

Overall significance level = 0,05

Comparisons for factor: Col 1

Comparison	Diff of Means	t	P	P<0,050
CN vs. CP	4,458	102,058	<0,001	Yes
TMP vs. CP	3,976	91,037	<0,001	Yes
CN vs. TMP	0,481	11,021	<0,001	Yes

Streptococcus mutans BIOFILME SIMPLES**One Way Analysis of Variance****Data source:** Data 1 in c13 ca cfu

Dependent Variable: Col 2

Normality Test (Shapiro-Wilk) Passed (P = 0,847)**Equal Variance Test:** Passed (P = 0,084)

Group Name	N	Missing	Mean	Std Dev	SEM
CN	3	0	6,983	0,170	0,0980
CP	3	0	2,290	0,196	0,113
TMP	3	0	2,521	0,548	0,316

Source of Variation	DF	SS	MS	F	P
Between Groups	2	41,991	20,995	171,441	<0,001
Residual	6	0,735	0,122		
Total	8	42,725			

The differences in the mean values among the treatment groups are greater than would be expected by chance; there is a statistically significant difference (P = <0,001).

Power of performed test with alpha = 0,050: 1,000

All Pairwise Multiple Comparison Procedures (Holm-Sidak method):

Overall significance level = 0,05

Comparisons for factor: **Col 1**

Comparison	Diff of Means	t	P	P<0,050
CN vs. CP	4,693	16,426	<0,001	Yes
CN vs. TMP	4,462	15,616	<0,001	Yes
TMP vs. CP	0,232	0,810	0,449	No

Candida albicans BIOFILMES SIMPLES X MISTO**One Way Analysis of Variance**

Data source: Data 1 in c13 ca cfu

Dependent Variable: Col 2

Normality Test (Shapiro-Wilk) Passed (P = 0,225)

Equal Variance Test: Passed (P = 0,356)

Group Name	N	Missing	Mean	Std Dev	SEM
CN	3	0	6,227	0,142	0,0823
CP	3	0	1,750	0,0293	0,0169
TMP	3	0	5,915	0,0888	0,0513
CN M	3	0	7,343	0,0366	0,0211
CP M	3	0	2,888	0,00520	0,00300
TMP M	3	0	6,861	0,0849	0,0490

Source of Variation	DF	SS	MS	F	P
Between Groups	5	78,471	15,694	2503,768	<0,001
Residual	12	0,0752	0,00627		
Total	17	78,546			

The differences in the mean values among the treatment groups are greater than would be expected by chance; there is a statistically significant difference (P = <0,001).

Power of performed test with alpha = 0,050: 1,000

All Pairwise Multiple Comparison Procedures (Holm-Sidak method):

Overall significance level = 0,05

Comparisons for factor: Col 1

Comparison	Diff of Means	t	P	P<0,050
CN M vs. CP	5,593	86,517	<0,001	Yes
TMP M vs. CP	5,111	79,070	<0,001	Yes
CN vs. CP	4,477	69,264	<0,001	Yes
CN M vs. CP M	4,454	68,907	<0,001	Yes
TMP vs. CP	4,165	64,427	<0,001	Yes
TMP M vs. CP M	3,973	61,461	<0,001	Yes
CN vs. CP M	3,339	51,654	<0,001	Yes
TMP vs. CP M	3,026	46,817	<0,001	Yes
CN M vs. TMP	1,428	22,090	<0,001	Yes
CP M vs. CP	1,138	17,610	<0,001	Yes
CN M vs. CN	1,115	17,253	<0,001	Yes
TMP M vs. TMP	0,947	14,643	<0,001	Yes
TMP M vs. CN	0,634	9,807	<0,001	Yes
CN M vs. TMP M	0,481	7,447	<0,001	Yes
CN vs. TMP	0,313	4,837	<0,001	Yes

Streptococcus mutans BIOFILMES SIMPLES X MISTO**One Way Analysis of Variance**

Data source: Data 1 in c13 ca cfu

Dependent Variable: Col 2

Normality Test (Shapiro-Wilk) Passed (P = 0,512)

Equal Variance Test: Failed (P < 0,050)

Test execution ended by user request, ANOVA on Ranks begun

Kruskal-Wallis One Way Analysis of Variance on Ranks

Data source: Data 1 in c13 ca cfu

Dependent Variable: Col 2

Group	N	Missing	Median	25%	75%
CN	3	0	6,663	6,630	6,669
CP	3	0	1,050	0,840	1,267
TMP	3	0	1,187	0,999	1,510
CN M	3	0	6,887	6,884	7,179
CP M	3	0	2,290	2,093	2,486
TMP M	3	0	2,548	1,961	3,055

H = 15,737 with 5 degrees of freedom. (P = 0,008)

The differences in the median values among the treatment groups are greater than would be expected by chance; there is a statistically significant difference (P = 0,008)

To isolate the group or groups that differ from the others use a multiple comparison procedure.

All Pairwise Multiple Comparison Procedures (Student-Newman-Keuls Method)

Comparison	Diff of Ranks	q	P<0,05
CN M vs CP	42,000	4,542	Yes
CN M vs TMP	39,000	5,035	Yes
CN M vs CP M	24,000	3,843	Yes
CN M vs TMP M	21,000	4,427	Yes
CN M vs CN	9,000	2,777	Yes
CN vs CP	33,000	4,260	Yes
CN vs TMP	30,000	4,804	Yes
CN vs CP M	15,000	3,162	No
CN vs TMP M	12,000	3,703	Do Not Test
TMP M vs CP	21,000	3,363	No
TMP M vs TMP	18,000	3,795	Do Not Test
TMP M vs CP M	3,000	0,926	Do Not Test
CP M vs CP	18,000	3,795	Do Not Test
CP M vs TMP	15,000	4,629	Do Not Test
TMP vs CP	3,000	0,926	Do Not Test

Note: The multiple comparisons on ranks do not include an adjustment for ties.

A result of "Do Not Test" occurs for a comparison when no significant difference is found between the two rank sums that enclose that comparison. For example, if you had four rank sums sorted in order, and found no significant difference between rank sums 4 vs. 2, then you would not test 4 vs. 3 and 3 vs. 2, but still test 4 vs. 1 and 3 vs. 1 (4 vs. 3 and 3 vs. 2 are enclosed by 4 vs. 2: 4 3 2 1). Note that not testing the enclosed rank sums is a procedural rule, and a result of Do Not Test should be treated as if there is no significant difference between the rank sums, even though one may appear to exist.